Positron emission tomography myocardial perfusion and glucose metabolism imaging

Josef Machac, MD,[a] Stephen L. Bacharach, PhD,[b] Timothy M. Bateman, MD,[b] Jeroen J. Bax, MD,[b] Robert Beanlands, MD,[b] Frank Bengel, MD,[b] Steven R. Bergmann, MD, PhD,[b] Richard C. Brunken, MD,[b] James Case, PhD,[b] Dominique Delbeke, MD,[b] Marcelo F. DiCarli, MD,[b] Ernest V. Garcia, PhD,[b] Richard A. Goldstein, MD,[b] Robert J. Gropler, MD,[b] Mark Travin, MD,[b] Randolph Patterson, MD,[b] Heinrich R. Schelbert, MD[b]

INTRODUCTION

Cardiac positron emission tomography (PET) imaging is a well-validated, reimbursable means to assess myocardial perfusion, left ventricular (LV) function, and viability. Presently, there is a proliferation of PET and PET/computed tomography (CT) instrumentation as well as an increase in educational programs that specifically address PET and PET/CT imaging. Technologists performing PET scans as well as physicians interpreting them should have a sound knowledge of recommended standards for the performance, interpretation, and quality control (QC) of cardiac PET in order to provide accurate and clinically relevant information to referring physicians, facilitating optimal patient management.

These guidelines are an update of an earlier version of these guidelines that have been developed by the Quality Assurance Committee of the American Society of Nuclear Cardiology.[1,2] The task of the Committee has been to document state-of-the-art PET applications and protocols approved by experts in the field and distribute these protocols to the nuclear cardiology community. It is recognized that PET and PET/CT imaging is evolving rapidly and that these recommendations may need further revision in the near future.

Part 1, "Patient Preparation and Data Acquisition," addresses the instrumentation and protocols recommended to yield technically adequate and clinically meaningful cardiac PET scans. This section includes detailed explanations of patient preparation options, recommended QC parameters, and scan acquisition and processing techniques. Within this document, items judged to be required are indicated as such. "Preferred" means that the parameter value listed is expected to provide the best results and its selection is strongly recommended. "Standard" means that the parameter value listed represents methodology judged to be standard by the consensus of the committee; its utilization is recommended, but other techniques may also be valid. "Acceptable" means that the parameter value listed is a valid alternative to "Standard." Techniques termed "Optional" indicate that the parameter value listed may be used or another acceptable parameter may be substituted.

Part 2, "Interpretation and Reporting," provides a systematic approach to QC, display, interpretation, and reporting of cardiac PET scans. Both subjective and objective semiquantitative interpretive methods to evaluate myocardial perfusion and viability are described. The Committee recognizes that all of these options may not be available on computer workstations presently provided commercially. Therefore such recommendations may be considered as general guidelines to direct the nuclear physician's scan interpretation in a detailed and organized fashion.

This publication is designed to provide imaging guidelines for those physicians and technologists who are qualified in the practice of nuclear cardiology. Although care has been taken to ensure that information supplied is accurate, representing the consensus of experts, it should not be considered as medical advice or a professional service, since specific guidelines are partly instrument-dependent, and the technology of PET and PET/CT imaging is evolving rapidly. The imaging guidelines described in this publication should not be used in clinical studies at any institution until they have been reviewed and approved by qualified physicians and technologists from that institution.

PART 1: PATIENT PREPARATION AND DATA ACQUISITION

A. General Comments

There is now an extensive infrastructure in PET imaging, with more than 1000 installed PET and PET/CT cameras in North America, spurred by their successful use in clinical oncology. A large number of PET scanners are continuing to be installed. Myocardial PET perfusion imaging with rubidium 82, reimbursed by

Chair.[a] Member.[b]
J Nucl Cardiol 2006;13:e121-51.
1071-3581/$32.00

doi:10.1016/j.nuclcard.2006.08.009

Centers for Medicare & Medicaid Services (CMS) since 1995, can be performed with a commercially available Rb-82 generator, obviating the need for a cyclotron. All metropolitan areas in North America now have at least one commercial fluorine 18 fluorodeoxyglucose (FDG) supplier. FDG PET imaging is now reimbursed for myocardial viability imaging. More recently, CMS reimbursement became available for myocardial perfusion imaging with nitrogen 13 ammonia, for those centers that do have a cyclotron, that could until recently offer PET myocardial perfusion imaging only for patients who could afford to pay for the procedure or who participated in a funded research study. This has made cardiac PET imaging possible at many clinical institutions, with the use of dedicated PET and PET/CT systems. The widespread installation of PET/CT cameras represents another significant change. The use of CT for attenuation correction substantially shortens the acquisition time for a clinical study. The present guidelines try to address the use of PET/CT cameras as best as possible with present knowledge and experience. It should be borne in mind, however, that only a handful of centers use PET/CT cameras for cardiac imaging, with few published studies providing guidance. The field is undergoing a rapid evolution, and the present guidelines for PET/CT imaging may soon be superceded or modified with newer advances.

N-13 ammonia and Rb-82 are well-accepted myocardial perfusion agents[3-9] for rest and stress PET myocardial imaging or in combination with FDG for determination of viability. FDG uptake in the myocardium has been well validated as an indicator of myocardial viability.[10-12] The methods of acquiring perfusion images and FDG images are given in Part 1. The manner in which the obtained images are interpreted and used clinically are described in Part 2. Section B, subsection iii, of Part 1 describes N-13 ammonia perfusion acquisitions (Table 1), and section B, subsection iv, describes Rb-82 perfusion imaging (Tables 2-4). Section C of Part 1 (Tables 5-7) describes FDG imaging. Note that all information below is applicable only to adult patients.

Oxygen 15–labeled water is often considered the ideal tracer for measurement of myocardial blood flow. Its use is not covered in this document for two reasons. First, it is currently not a Food and Drug Administration–approved drug. Second, it does not usually produce clinically interpretable perfusion images. Instead, a (well-validated) mathematical model must be used to produce numeric values of flow in each region of the myocardium. Likewise, tracers of myocardial metabolism such as carbon 11 acetate, C-11 fatty acids, or tracers suitable for myocardial receptor imaging are not covered, due to their present investigational status.

We discuss only the use of so-called dedicated, multicrystal ring PET and PET/CT detector systems. We have not included coincidence gamma camera systems or (noncoincidence) collimated single photon emission computed tomography (SPECT) systems. Gamma camera coincidence systems ("hybrid" PET) were not considered, because it appeared that the impact of factors such as linearity of counts with activity, scatter correction, attenuation correction, and so on had not yet been addressed sufficiently to allow standardized guidelines to be proposed. Noncoincidence collimated SPECT with FDG presented a different problem. Collimated FDG imaging has the advantage of permitting simultaneous, dual-isotope perfusion and metabolism measurements, a valuable feature for viability measurements and a feature that is not possible with coincidence PET. Despite this advantage, relatively few institutions utilize noncoincidence FDG imaging. Therefore it is not clear that a "standard" method of acquisition could be determined at this time. Both gamma camera coincidence systems and 511-keV SPECT systems may well play a role in future cardiac FDG viability measurements. When a larger clinical experience has been gained, the development of guidelines for these modalities may prove worthwhile.

Attenuation effects are much more significant with PET than SPECT because the 511-keV photons are attenuated along the entire path between the two detectors connected by the coincidence circuit detecting an event. Therefore attenuation correction must be performed for accurate interpretation of PET images of an asymmetrical organ such as the heart. The algorithms to correct for attenuation are more accurate with PET than SPECT because the length of the path of attenuation is constant and known for PET (distance between any two detectors) and variable for SPECT. Accurate correction for attenuation represents a significant advantage of PET compared to SPECT, especially in patients with large body habitus. In addition, accurate attenuation correction and calibration of the PET systems allow for absolute measurements of radioactivity in selected regions of interest and absolute quantification of myocardial blood flow both at rest and during stress using compartmental modeling and kinetic analysis.

Various methods have been developed with measured attenuation using radioactive transmission sources, such as germanium 68. Typically, radioactive sources rotate around the patient while transmission images are acquired.

Several manufacturers are now offering integrated PET/CT imaging systems combining state-of-the-art dedicated PET tomographs side by side with multidetector CT units, with a common imaging bed. The CT units in these integrated systems were first offered with 2 and 4 rows of detectors, are now available with 8 and 16 rows of detectors, and will soon advance to 32 to 64 rows of

detectors, opening the horizon for cardiac applications combining myocardial perfusion and viability with calcium scoring and CT coronary angiography.[13] However, the latter applications are outside the scope of this review.

With these integrated systems, a CT scan and a PET scan can be acquired sequentially with the patient lying on the imaging table and simply being translated between the two systems. Accurate calibration of the position of the imaging table and the use of common parameters in data acquisition and image reconstruction permit the fusion of images of anatomy, perfusion, and metabolism from the same region of the body that are registered in space and only slightly offset in time. Because of the high photon flux of x-rays, the CT scan is actually a high-resolution transmission map. With proper care, these data can be used to perform a high-quality attenuation correction during image reconstruction of the emission data.

One advantage of CT attenuation maps over the radioactive sources is the short duration for acquisition of the transmission images, in the range of 10 to 60 seconds for one bed position over the heart. An adequate CT transmission map can actually be obtained with very low current (10 mA),[14] but the low resolution of these images makes them suboptimal for anatomical localization.

PET scanner instrumentation and design are continually evolving. New crystal materials such as lutetium oxyorthosilicate (LSO) and gadolinium oxyorthosilicate (GSO) are now available as well as others. These crystals have higher light output and shorter dead time than the conventional bismuth germanate (BGO) crystals but have reduced stopping power for 511-keV photons. For some manufacturers, LSO- and GSO-based systems have superceded their conventional BGO systems. In certain applications (eg, 3-dimensional [3D], septa-out imaging) systems with these new crystals may offer improved performance. In addition, changes in electronics, crystal/photo multiplier tube arrangements, and scatter and randoms corrections recently have been utilized to improve performance of BGO-based instruments in 3D mode. Designing a PET scanner always involves making choices and tradeoffs between various instrument characteristics (eg, sensitivity and scatter). As a result, there are variations in scanner characteristics between various models of machine from the same manufacturer, as well as between manufacturers.

Therefore Tables 1, 2, 3, 4, and 7 should only be taken as guides to appropriate image acquisition, not as representing hard-and-fast rules. This is especially true when assessing 3D versus 2-dimensional (2D) acquisitions, as well as when determining the appropriate number of total true events necessary to create a "good-quality image." It is critical for the user to have a good understanding of the characteristics of his or her PET scanner (eg, plots of noise-equivalent counts vs activity concentration, dead time and randoms measurements, scatter fraction) in order to know how the machine will behave under the circumstances of cardiac imaging. See, for example, "Performance Measurements of Positron Emission Tomographs" (NU 2-2001) from the National Electrical Manufacturers Association.[15]

Three-dimensional acquisition (ie, septa-out) is, in principle, many times more sensitive than 2D (septa-in). However, this often is only true at low doses. Randoms, dead time, and scatter can greatly reduce the effective sensitivity of 3D acquisitions and at high doses. Three-dimensional acquisitions can (depending on the scanner characteristics) actually produce poorer-quality images than 2D imaging for the same imaging time. Therefore in the past, when using 3D imaging with a BGO crystal camera, 3D imaging has often only been used when the dose must be minimized (eg, normal volunteers, in children, or when multiple studies are planned). The 3D acquisition of cardiac images is an option that should be considered only by those institutions that are able to carefully monitor and assess randoms, dead time, and scattered events. Note that 3D imaging is more practical with the advent of LSO- and GSO-based PET scanners and even with BGO scanners with new-generation optimized photo multiplier/crystal coupling schemes and high-speed electronics. Still, the use of 3D cardiac imaging with these new-generation machines remains to be fully characterized, and preliminary reports have been mixed. Use of 3D imaging is highly dependent on the ability to minimize and accurately correct for dead time, randoms, and scatter. Typically, there is much greater scatter with 3D (ie, septa-out) operation than with 2D (septa-in) operation, for all crystal types. The newer crystals (LSO or GSO) and newer-generation electronics (with BGO) may, in principle, permit reduction of randoms and dead time and therefore may permit shorter imaging time to be achieved. The degree to which any of these improvements can be achieved in practice for cardiac imaging remains unknown at this writing. Scatter remains much higher in 3D mode than in 2D mode even for new-generation 3D machines. The user must carefully evaluate plots of noise-equivalent counts and other system parameters to determine the optimum dose of FDG in 3D mode. Note that some new scanners only permit septa-out operation.

B. PET Perfusion Imaging: N-13 Ammonia and Rb-82

N-13 ammonia has been used in scientific investigations in cardiac PET imaging over the past two

decades. Recently, its use has been approved for clinical imaging. Its 10-minute half-life requires an onsite cyclotron and radiochemistry synthesis capability. The N-13 nitrogen decays by positron emission. The daughter product is C-13 carbon, which is stable. Myocardial uptake of N-13 ammonia depends on flow, extraction, and retention. First-pass myocardial extraction of N-13 ammonia is very high (95%).[16] Following this initial extraction across the capillary membrane and via passive diffusion into the myocyte, N-13 ammonia is either incorporated into the amino acid pool as N-13 glutamine or back-diffuses into the blood. The myocardial tissue retention is an adenosine triphosphate–dependent metabolic process.[17] Thus uptake and retention can both be altered by changes in the metabolic state of the myocardium. A suggested acquisition protocol is given in Table 1, which can be performed by a wide variety of PET gamma cameras.

The radiation dosimetry from N-13 ammonia in an adult is 0.148 rad total effective dose from 20 mCi.[18] The critical organ is the urinary bladder, which receives 0.60 rad from 20 mCi.[19] The dosimetry is relatively low, due to the short half-life of N-13 and the low energy of the emitted positrons.

Rb-82 is a monovalent cationic analog of potassium and is produced in a commercially available generator by decay from strontium 82 attached to an elution column. Sr-82 has a half-life of 25.5 days and decays to Rb-82 by electron capture. Rb-82 is eluted from the generator with saline. Rb-82 decays with a physical half-life of 75 seconds by emission of a positron. The daughter product is krypton 82, which is stable. The Sr-82–containing generator is replaced every 4 weeks.

Rb-82 is eluted with 10 to 50 mL normal saline by a computer-controlled elution pump, connected by intravenous (IV) tubing to the patient. While the generator is fully replenished every 10 minutes, experiments have shown that 90% of maximal available activity can be obtained within 5 minutes after the last elution.[20] Thus, serial imaging can be performed every 5 to 6 minutes. While the short half-life of Rb-82 taxes the performance limits of PET scanners, it facilitates the rapid completion of a series of resting and stress myocardial perfusion studies. Rb-82 is a very efficient imaging agent for routine clinical usage.

Rb-82 is extracted from plasma with high efficiency by myocardial cells via the Na^+/K^+ adenosine triphosphatase pump. Myocardial extraction of Rb-82 is similar to thallium 201[21,22] and less than N-13 ammonia. Extraction decreases with increasing blood flow.[23,24] Rb-82 extraction can be decreased by severe acidosis, hypoxia, and ischemia.[25-27] Thus, uptake of Rb-82 is a function of blood flow, metabolism, and myocardial cell integrity.

Acquisition protocols for different types of PET scanners are shown in Tables 2, 3, and 4. The short half-life of Rb-82 poses a challenge for achieving optimal image quality. For that reason, optimal acquisition parameters differ among the several main types of PET scanners. Because of the short half-life of Rb-82 and the need for the patient to lie still in the camera during the study, stress imaging of this agent is limited to pharmacologic stress, although studies have obtained serviceable Rb-82 images with supine bicycle exercise or even treadmill exercise.[28]

i. **Preparation.** Patient preparation is similar to preparation for stress and rest myocardial SPECT imaging (Tables 1-4). This includes an overnight fast of 6 hours or more, avoidance of caffeinated beverages for at least 12 hours, and avoidance of theophylline-containing medications for 48 hours.[29]

ii. **Stress testing.** This document does not address methods for performing stress studies (eg, protocols for administration of pharmacologic stress agents). These protocols are, for the most part, generic for all perfusion agents.[29] The specific differences in acquisition protocols for N-13 ammonia or Rb-82 imaging are related to the duration of uptake and clearance by these radiopharmaceuticals and their physical half-lives.

iii. **N-13 ammonia acquisition protocol: Introduction to Table 1.** Table 1 summarizes the recommended guidelines for performing N-13 ammonia perfusion scans with dedicated, multicrystal PET or PET/CT cameras for rest and stress myocardial PET perfusion imaging for diagnosis or evaluation of coronary artery disease (CAD) or as part of an assessment of myocardial viability. N-13 ammonia is a valuable agent for measuring either absolute or relative myocardial blood flow.[3,4,6-9] For measurements of absolute flow, dynamic acquisition from time of injection is required, followed by fitting to one of several possible physiologic models. Absolute flow measurements will not be discussed here, because they are time-consuming and require a high level of expertise, which has led to their being performed primarily in a research setting. Relative perfusion measurements, described below, are often used clinically in the evaluation of myocardial perfusion at rest and stress or in the determination of viability. Methods for normalizing and interpreting these images are discussed in Part 2 below.

Notes for Table 1

1. Uptake is relatively rapid (typically often nearly complete in 90 seconds), and radioactive decay (10-minute half-life) is fast. Typically, uptake images are acquired no sooner than about 90 seconds after the end of infusion. Therefore a very slow infusion will require static imaging to be delayed, potentially

Table 1. N-13 ammonia cardiac perfusion studies

Feature		Technique	For details, see note in text
Patient preparation	Overnight fast (>6 h)	Preferred	
	No caffeine or caffeinated beverages for 12 h	Acceptable	
	No theophylline-containing medications for 48 h	Preferred	
Dose	10-20 mCi (typical) (370-740 MBq)	Standard	1
	Bolus or <30-s infusion	Preferred	1
Imaging acquisition	Static	Standard	
	Start time: 1.5-3 min after end of infusion	Standard	2
	Duration: 5-15 min	Standard	3
Pixel size (reconstructed)	2-3 mm	Preferred	4
	4 mm	Optional	
Attenuation correction			
PET	Measured attenuation correction: immediately before scan	Standard	5
	Measured attenuation correction: immediately after scan	Optional	5
PET/CT	CT-based measured attenuation correction: immediately after scan	Standard	5
Reconstruction method	FBP or iterative expectation maximization (eg, OSEM)	Standard	4
Gating	ECG gating of myocardium	Preferred	6
Patient positioning	Arms out	Preferred	7
	Arms in (but no movement)	Optional	7
Calcium scoring	Gated CT acquisition separate from CTAC	Optional	8

resulting in count loss because of the 10-minute half-life. Large patients may benefit from higher (25-30 mCi) doses.

2. The static image should not include the initial rapidly changing uptake portion of the study. Therefore a minimum of 90 seconds should typically elapse between the end of infusion and the beginning of the static scan. In fact, the arterial blood concentration of ammonia is often still quite significant even at 90 seconds after a rapid bolus injection. Nonetheless, many published data are based on only a 90-second delay before the start of imaging.
3. After an initial period of rapidly changing activity levels during the uptake period, the decay-corrected ammonia concentration subsequently usually changes only very slowly. However, the 10-minute N-13 half-life makes acquisition duration longer than 20 minutes of limited value unless total counts are very low.
4. It is desirable to keep reconstruction parameters similar to those used for the FDG portion of a viability study (see notes for Table 7) in order that perfusion and metabolism are affected by reconstruction parameters in the same way. This permits more accurate comparison between the two image sets.
5. Measured attenuation by a rotating 511-keV source is preferred for dedicated 2D scanners. Either prescan or postscan is satisfactory, providing it has been verified that the user's attenuation correction software can adequately correct for residual emission activity. Attenuation correction simultaneous with emission scan is not recommended unless data become available to indicate that the high count rate and rapidly changing distribution of the isotope will not adversely affect the transmission scan. See notes on attenuation correction in Table 7. For patients undergoing PET/CT, two separate CT-based transmission scans should be performed for correction of the rest scan (either before or after the emission scan) and stress (after the emission scan is preferred to prevent misregistration artifacts on the corrected ammonia images).
6. If myocardial wall motion information is desired, it is indeed possible to achieve sufficiently high-quality gated ammonia scans to accurately evaluate wall motion and ejection fraction (EF).[30]
7. Ideally, the patient should be positioned supine, with the arms out of the camera field of view. This can be tolerated by nearly all patients, provided some care is given to a method to support the arms. Alternatively, an overhead bar has often been used as a hand-hold

Table 2. Rb-82 rest/stress myocardial perfusion imaging guideline for BGO PET imaging systems

Feature		Technique	For details, see note in text
2D dose: BGO systems	40-60 mCi (1480-2220 MBq)	Standard	1
3D dose: BGO systems	10-20 mCi (370-740 MBq)	Optional	1
Patient positioning			
PET	Use scout scan: 10-20 mCi Rb-82 (370-740 MBq)	Standard	2
	Use transmission scan	Optional	2
PET/CT	CT scout	Standard	2
Injection rate	Bolus of ≤30 s	Standard	
Imaging time	3-6 min	Standard	3
Imaging delay after injection	LVEF >50% = 70-90 s	Acceptable	3
	LVEF <50% = 90-130 s		
	130-150 s if LVEF is not known	Optional	
Imaging mode	Phased/dynamic (no delay after injection)	Preferred	3
	Gated acquisition (delay after injection)	Optional	
Rest attenuation correction	Measured attenuation correction, before or after	Standard	4
Stress testing	Pharmacologic agents	Standard	5
Stress attenuation correction			
PET	Measured attenuation correction before or after stress to ensure image registration	Optional	6
PET/CT	Measured attenuation correction after stress to ensure image registration	Standard	6
Reconstruction method	FBP or iterative expectation maximization (eg, OSEM)	Standard	7
Reconstruction filter	Sufficient to achieve desired resolution/smoothing, matched stress to rest	Standard	7
Pixel size (reconstructed)	2-3 mm	Preferred	7
Coronary calcium scoring	Gated CT acquisition separate from CTAC	Optional	8

for arm support. In those very few cases in which arms-out positioning is not possible (eg, patients with very severe arthritis), the arms can be in the field of view. In this case the transmission scan time may have to be increased, and it is of critical importance that the arms not move between transmission and emission, or artifacts will result. Note that when performing ammonia/FDG perfusion/metabolism studies, it is best to keep patient positioning similar for both studies, and this is often very difficult or impossible to accomplish with a change (arms in/out) in arm position. In patients undergoing PET/CT imaging, arms in (down) the field of view result in beam-hardening artifacts on the CT-based transmission scan, which usually lead to streak artifact of the corrected emission scans.

8. With PET/CT systems, it is possible to acquire a separate (from the CT-based attenuation correction [CTAC]) gated CT with adequate breath-holding for measuring coronary calcium scores. Calcium scores provide a measure of atherosclerotic burden that, in combination with the stress perfusion PET images, may be useful to guide patient management. However, because the added prognostic value of this approach has not been proven, calcium scoring remains optional.

iv. **Rb-82 perfusion acquisition protocol. Introduction to Tables 2, 3, and 4**. Tables 2, 3, and 4 summarize the acquisition parameters necessary to acquire an Rb-82 perfusion study with a dedicated PET or PET/CT camera.[4,9] Because of the divergent operating characteristics of BGO, LSO, and GSO PET imaging systems, recommendations are considered separately for each type of system.

Notes for Tables 2 and 3

1. Scout scanning: Scout scanning is recommended before each injection to ensure that the patient is correctly positioned and is not unnecessarily exposed to radiation. This can be done with a fast transmission image or with a low-dose Rb-82 injection (10-20 mCi).

Table 3. Rb-82 rest/stress myocardial perfusion imaging guideline for LSO PET imaging systems

Feature		Technique	For details, see note in text
3D dose: LSO systems	30-40 mCi (1110-1480 MBq)	Standard	1
2D dose: LSO systems	40-60 mCi (1480-2220 MBq)	Optional	1
Patient positioning			
PET	Use scout scan: 10-20 mCi Rb-82 (370-740 MBq)	Preferred	2
	Use transmission scan	Optional	2
PET/CT	CT scout	Standard	2
Injection rate	Bolus of ≤30 s	Standard	2
Imaging time	3-6 min	Standard	3
Imaging delay after injection	LVEF >50% = 70-90 s	Acceptable	3
	LVEF <50% = 90-130 s		
	130-150 s if LVEF is unknown	Optional	
Imaging mode	Phased/dynamic (no delay after injection)	Preferred	3
	Gated acquisition (delay after injection)	Optional	
Rest attenuation correction	Measured attenuation correction, before or after	Standard	4
Stress testing	Pharmacologic agents	Standard	5
Stress attenuation correction			
PET	Measured attenuation correction before or after stress to ensure image registration	Optional	6
PET/CT	Measured attenuation correction after stress to ensure image registration	Standard	6
Reconstruction method	FBP or iterative expectation maximization (eg, OSEM)	Standard	7
Reconstruction filter	Sufficient to achieve desired resolution/smoothing, matched stress to rest	Standard	7
Pixel size (reconstructed)	2-3 mm	Preferred	7
Coronary calcium scoring	Gated CT acquisition separate from CTAC	Optional	8

Note that the low-dose Rb-82 scout scan is also used to estimate circulation times and cardiac blood pool clearance times, which assist in selection of the optimum injection to imaging delay time between Rb-82 injection and initiation of acquisition of myocardial Rb-82 images (see 3 below). With PET/CT systems, the CT scout scan is routinely used for patient positioning.

2. General dose considerations: In determining appropriate patient dosages,[5] the following issues should be considered: (a) Patient exposure is typically low relative to SPECT because of the short half-life of the isotope. (b) Staff exposure could be high unless care is taken to avoid close proximity to the generator and the patient during injection, because of the limited effectiveness of shielding and the higher dosages used in Rb-82 PET. (c) Three-dimensional imaging requires less dosage than 2D imaging because of the improved sensitivity of the system; however, the dead time and increased randoms of the camera may not allow one to utilize the improved sensitivity. (d) In addition, the very large increase in scattered events may also obviate some of the sensitivity advantages of 3D imaging. Newer imaging crystals (eg, LSO, GSO, and others) allow imaging at higher count rates, as does the new generation of electronics coupled with BGO systems. Count rate issues are especially critical to Rb-82 imaging.

   NOTE: See previous discussion of 2D versus 3D imaging. For Rb-82 imaging, 3D imaging, even with new-generation scanners, must be used with care.

3. Rest imaging time: Rest imaging should be performed before stress imaging to reduce the impact of residual stress effects (eg, stunning, steal). About 80% of the useful counts are acquired in the first 3 minutes, 95% of the useful counts are obtained in the first 5 minutes, and 97% are obtained in the first 6 minutes. The patient should be infused with Rb-82 for a maximum of 30 seconds. After the dose is delivered, patients with normal ventricular function (LVEF >50%) are typically imaged starting 70 to 90 seconds after the

injection. For those with reduced ventricular function (LVEF 30%-50%), imaging usually is begun 90 to 110 seconds after termination of the infusion, and those with poor function (LVEF <30%) are typically imaged at 110 to 130 seconds. These times can be estimated from observations of the scout Rb-82 scan, if used. Ideally, patients should be imaged by a dynamic acquisition to allow for retrospective removal of phases that have Rb-82 in the blood pool, in which case imaging can begin within a few seconds after the start of the rubidium infusion. Excessive blood pool counts can scatter into myocardial defects, making them artifactually look milder and thus potentially reversible. Excessive blood pool counts can also make the LV cavity appear smaller, especially at rest, leading to a false perception of LV cavity dilatation during stress. The dynamic data set is also useful to estimate coronary flow reserve. Electrocardiographic (ECG) gating can also be used with Rb-82. Images can be acquired by 2D or 3D imaging modes (but see 2D vs 3D notes to Table 7). If simultaneous ECG gating is used, the standard delay delineated above is applied. List mode acquisitions, which allow for simultaneous phase/dynamic and ECG-gated acquisitions, are optional as tools for sorting and reconstruction of list mode data but are not yet ready for routine clinical use.

4. Rest transmission imaging: Rb-82 myocardial perfusion should only be performed with attenuation correction.[31] Attenuation correction can be accomplished with a rotating line source in a dedicated PET system or with CT in a PET/CT system.
   a. Dedicated PET: Two techniques are typically used for creating the patient-specific transmission maps: direct measurement of patient attenuation with a rotating line source of either Ge-68 or cesium 137 or segmentation of patient-specific attenuation maps. The former are very sensitive to the choice of reconstruction algorithm and, depending on reconstruction algorithm used, could require 60 to 600 seconds' acquisition time to produce a reasonable attenuation map.[32] 2D imaging generally requires longer attenuation map imaging time compared to 3D imaging. Segmentation algorithms are relatively insensitive to noise but are very dependent on the quality of the program used for performing the transmission scan segmentation and are influenced by lung attenuation inhomogeneities (eg, partial-volume effects from liver). Transmission data are typically performed sequentially, so it is essential that the patient remain still between transmission and emission images. Many laboratories perform the transmission scan between the rest and stress images, although some perform the transmission scan at the very beginning. Loghin et al[33] have determined that if the transmission scan is performed in the beginning of the study, greater misregistration occurs with the later stress images, possibly due to gradual upward creep of the diaphragm, due to pressure from visceral fat.
   b. CT based: For PET/CT systems, x-ray computed tomography can be used for acquiring a transmission map for attenuation correction. This technique may be advantageous because the transmission map can be acquired rapidly (15-60 seconds), can be repeated for rest and stress and metabolic imaging, and has independent diagnostic information, such as coronary calcium visualization and non-cardiac anatomic information. To acquire a CT-based transmission scan, it is necessary to first acquire a planar scout CT acquisition. This scan is used to measure the axial limits of the CT acquisition. Following this acquisition, the CT transmission scan is acquired. The best approach for CT transmission imaging is still evolving, and therefore this guideline can only suggest some considerations. Some of the considerations for CT scanning are as follows:
      i. If CT is either for attenuation correction or anatomical evaluation, this will have an effect on the kV and mAs used in the acquisition. A transmission scan usually requires only a low CT current, as opposed to calcium scoring or CT angiography, which require higher CT currents. An effort must be made to minimize radiation exposure.
      ii. Breathing protocols are not clearly settled. Data seem to be in favor of free breathing and a slow CT scan. Current practice discourages breath-holding, particularly in end inspiration because of its potential for causing uncorrectable misregistration. A very rapid transmission CT scan performed at the same speed as for whole-body PET/CT images frequently produces artifacts at the lung-liver interface and can sample parts of the heart and diaphragm in different positions, causing misregistration and an artifact where pieces of the diaphragm appear to be suspended in the lung. Although specifics vary among laboratories, the duration of the CT transmission scan is typically from 10 to 60 seconds.
      iii. Metal artifacts can present a challenge for the reconstruction algorithm and must be

Table 4. Rb-82 rest/stress myocardial perfusion imaging guideline for GSO PET imaging systems

Feature		Technique	For details, see note in text
3D dose: GSO systems	20 mCi (740 MBq)	Standard	1
Patient positioning			
PET	Use scout scan: 10-20 mCi Rb-82 (370-740 MBq)	Standard	2
	Use transmission scan	Optional	2
PET/CT	CT scout	Standard	2
Injection rate	Bolus of ≤30 s	Standard	
Imaging time	3-6 min		3
Imaging delay after injection	2-3 min (when count rate reaches 10-11 million cps)	Standard	3
Imaging mode	Phased/dynamic (no delay after injection)	Standard	4
Gated imaging	None		4
Rest attenuation correction	Measured attenuation correction, before or after	Standard	5
Stress testing	Pharmacologic agents	Standard	
Stress attenuation correction			
PET	Measured attenuation correction with stress to ensure image registration	Optional	5
	CT transmission scan	Optional	
PET/CT	Measured attenuation correction after stress to ensure image registration	Standard	5
Reconstruction method	Iterative (RAMLA)	Standard	6
Reconstruction filter	None	Standard	7
Pixel size (reconstructed)	4	Standard	
Coronary calcium scoring	Gated CT acquisition separate from CTAC	Optional	8

compensated for to produce accurate attenuation maps.[34,35]

5. Stress testing: The long infusion time for Rb-82 and slow uptake require some modifications to conventional stress testing. On average, the patient should remain at peak stress for somewhat longer than conventional SPECT-based radionuclide stress testing. The radionuclide should be injected in a manner such that all of the Rb-82 is taken up in the stress state. See previously published guidelines for further information on pharmacologic agents for stress testing.[29]
6. Stress transmission imaging: These images should be acquired while the patient is still at the peak of stress. If the patient cannot tolerate this or if the stress testing protocol will not allow this, the technologist and physician must carefully inspect the transmission and emission data sets to ensure that they are properly registered in the transaxial, sagittal, and coronal planes. For patients undergoing PET/CT, a separate CT-based transmission scan for correction of the stress rubidium images is standard. A post-stress transmission scan is preferred to minimize misregistration artifacts on the corrected Rb-82 images when misregistration compensation software is not available.
7. Processing protocol: Several corrections are required for creating data sets that can be used for reconstruction. Rb-82 data must be corrected for randoms, scatter, dead time, attenuation, and decay before reconstruction can begin. Once these corrections are applied, the data can be reconstructed with either filtered backprojection (FBP) or iterative algorithms. For viability studies, it is often desirable to match the resolution of the FDG and the perfusion (rubidium) agent, although this is less critical when the data are divided into 8 or fewer sectors per short-axis slice and comparisons made on a sector-by-sector basis. For rest/stress comparisons, the rest/stress images must have matched resolution. Filtering with FBP or additional filtering of the ordered-subset expectation maximization (OSEM) (eg, Butterworth, Hanning, Gaussian) is usually necessary to achieve adequate noise properties. Again, care must be taken to match reconstructed resolution when making pixel-by-pixel comparisons of perfusion and metabolism.
8. With PET/CT systems, it is possible to acquire a separate gated CT with breath-holding for measuring

coronary calcium scores. Calcium scores provide a measure of atherosclerotic burden that, in combination with the stress perfusion PET images, may be useful to guide patient management. However, because the added prognostic value of this approach has not been proven, calcium scoring remains optional.

Notes for Table 4

1. Given the higher sensitivity of the 3D imaging obligatory in existing GSO systems, a lower dose of Rb-82 is sufficient and preferred to reduce dead time and randoms. Radiation exposure is further decreased.
2. The existing GSO systems have not featured gated acquisition until recently.
3. The GSO system uses a Cs-137 rod source to acquire a transmission scan for attenuation correction. A CT transmission scan is an alternative for GSO PET/CT systems.
4. The GSO system uses the RAMLA reconstruction technique (row action maximum likelihood algorithm).
5. For the GSO system, there should not be any reconstruction filter. (The RAMLA/Blob includes a texture/filter factor.)

C. PET FDG Metabolism Imaging

i. **Background and FDG tracer characteristics.** Tables 5, 6, and 7 summarize the recommended guidelines for performing cardiac FDG scans with dedicated, multicrystal PET and PET/CT cameras, as part of an assessment of myocardial viability. Tables 5 and 6 summarize the patient preparation and method of FDG administration. Table 7 discusses the image acquisition.

Preserved metabolism for the production of adenosine triphosphate is one of the critical features of myocardial viability. FDG is F-18–labeled 2-deoxyglucose, an analog of glucose. It is the principal workhorse in clinical PET viability imaging. F-18 is produced in a cyclotron through the (p,n) reaction, consisting of bombardment of O-18–enriched water.[36]

F-18 fluorine decays by the emission of a positron with a half-life of 109.8 minutes, whereby F-18 fluorine is converted into O-18 oxygen. The low kinetic energy of the positron, 635 keV, allows the highest spatial resolution among all PET radionuclides. The whole body dosimetry from a 10-mCi dose is 0.7 rem,[37] as compared to 2.0 rem from a 3.5-mCi dose of Tl-201[38] and 0.5 rem from a 30-mCi dose of Tc-99m sestamibi.[39] For FDG, the critical organ is the urinary bladder, which receives 5.9 rem.

FDG is an analog of glucose and is used as a tracer of glucose metabolism. FDG enters into the cells by the same transport mechanism as glucose and is phosphorylated intracellularly by a hexokinase into FDG-6-phosphate (FDG-6-P). In tissues with a low concentration of glucose-6-phosphatase, such as the myocardium, FDG-6-P does not enter into further enzymatic pathways and accumulates intracellularly proportionally to the glycolytic rate of the cell. The myocardium can use various substrates according to substrate availability, hormonal status, and other factors. In a typical fasting state, the myocardium primarily utilizes free fatty acids, but post-prandially or after a glucose load, it favors glucose.[40,41]

Following injection, FDG is slowly taken up by body tissues, including the myocardium. Imaging is performed about 45 to 90 minutes after injection. The 110-minute physical half-life of F-18 FDG allows sufficient time for synthesis and purification, its commercial distribution in a radius of several hours from the production site, its temporary storage at the user site, the absorption time after injection, and sufficient imaging time to yield images of high quality.

ii. **Patient preparation: Introduction to Tables 5 and 6.** FDG uptake, combined with a PET or SPECT perfusion measurement, has been well validated as a measure of myocardial viability (see Part 2 of these guidelines). FDG uptake begins with facilitated diffusion, followed by hexokinase-mediated phosphorylation. Therefore, uptake of FDG requires viable myocardial cells. In the fasting state, normal myocardium preferentially utilizes free fatty acids. The uptake of glucose and FDG is generally low, although fairly variable. In the fasting state, uptake inhomogeneity frequently occurs. Therefore, whereas uptake of FDG indicates viability, lack of uptake could either indicate nonviable tissue or indicate viable tissue that was utilizing substrates other than glucose. For this reason, every effort is made to force the myocardium to utilize primarily glucose to meet its energy needs by stimulating a natural insulin response. This is usually accomplished by having the patient fast for at least 6 hours and then administering a standardized glucose load, either orally or intravenously. Subsequent to glucose loading, glucose and insulin plasma levels are elevated, and glucose is the preferred substrate for energy metabolism.[42] The approach is outlined in Table 5.

There are several approaches to the administration of glucose. The guiding principle seems to be that the blood glucose (BG) needs to be increased by glucose administration (in order to shift myocardial metabolism to glucose) and, then, to be declining (to promote FDG uptake) after insulin injection before FDG administration. The situation is more complicated should the patient be diabetic, not achieve a sufficiently low fasting BG level, or have too high a BG level after glucose admin-

Table 5. FDG cardiac PET: Patient preparation guidelines—An overview

Procedure		Technique	For details, see note(s) in text
Fasting period	Step 1: Fast patient		1
	6-12 h	Preferred	1
	<6 h	Suboptimal	1
	Step 2: Check blood glucose and then glucose load (choose one of the following 4 options)		
Oral glucose load	Option 1: Oral glucose loading		
	IF: fasting BG < ~110 mg/dL AND: No known diabetes THEN: (1) Oral glucose load: typically 25-100 g orally (see Table 6) (2) Monitor blood glucose (see Table 6)	Standard	1 and 2, as well as Table 6
	IF: fasting BG > ~110-130 mg/dL OR: Known diabetes THEN: See Table 6	Standard	1, 2, 4, and 5
	OR		
IV, protocol A	Option 2: Hyperinsulinemic/euglycemic IV clamp	Optional	
	For details, see sample protocol A		4
	OR		
IV, protocol B	Option 3: Dextrose IV infusion	Optional	5
	For details, see sample protocol B		
	OR		
	Option 4: Acipimox		
Acipimox	Acipimox, 250 mg orally (see reference in note 3 for details), not available in United States		3
	Step 3: Administer FDG		
FDG injection	Time: Dependent on which option was selected	Standard	Table 7, item 1
	Administer FDG intravenously; see Table 7, item 1, for details		
	Step 4: Begin imaging		
Begin PET imaging	Time 60-90 min post FDG injection: start imaging, see Table 7		Table 7

istration. There are a variety of methods to deal with these situations. Table 6 discusses several options should BG values not reach the desired ranges. In addition, two sample IV protocols (protocol A and protocol B) are given below. These protocols illustrate some of the various possible approaches to IV glucose loading and BG level control. Some of the glucose-loading methodologies are easily implemented in standard nuclear medicine facilities, whereas others may be more elaborate than some facilities feel comfortable performing on a routine basis. Most laboratories utilize the oral glucose–loading methods, with supplemental insulin if needed, because of its simplicity. The reader is urged to examine Tables 5 and 6 and the sample protocols and use them as a guide to developing an approach that will be feasible in his or her own setting.

Notes for Tables 5 and 6: Patient Preparation

1. **Myocardial substrate utilization.** As mentioned in the introduction to Tables 5 and 6, for evaluation of myocardial viability using FDG, the substrate and hormone levels in the blood need to be pushed to favor utilization of glucose by the myocardium.[11,43] This is usually accomplished by loading the patient with glucose after a fasting period of at least 6 hours to induce an endogenous insulin response. A shorter fasting time may depress this physiological response. The most common method of glucose loading is with an oral load of 25 to 100 g, but IV loading is also used and has some advantages (as described in detail in the two sample protocols below). Either can be adequate for nondiabetic patients, if BG level falls sufficiently (see Table 6 for details) before FDG injection. The IV

Table 6. Guidelines for BG maintenance (eg, after oral glucose administration) for optimal FDG cardiac uptake, BG of approximately 100 to 140 mg/dL at FDG injection time

BG at 45-60 min after administration	Possible restorative measure	Technique	For details, see note(s) in text
130-140 mg/dL	1 u regular insulin	Standard	1 and 2
140-160 mg/dL	2 u regular insulin		
160-180 mg/dL	3 u regular insulin		
180-200 mg/dL	5 u regular insulin		
>200 mg/dL	Notify physician		

route avoids potential problems due to variable gastrointestinal absorption times or inability to tolerate oral dosage. Note that if the patient is taking medications that may either antagonize or potentiate the effects of insulin, these should be taken into account by the physician.

2. **Diabetic patients.** Diabetic patients pose a challenge, either because they have limited ability to produce endogenous insulin or because their cells are less able to respond to insulin stimulation. For this reason, the simple fasting/oral glucose–loading paradigm is often not effective in diabetic patients. Fortunately, use of insulin along with close monitoring of BG (Table 6) yields satisfactory results.[44] Image improvement can also be seen after waiting 2 to 3 hours after injection before imaging (at the expense of increased decay of the radiopharmaceutical FDG). An alternative method is the euglycemic hyperinsulinemic clamp,[45] a rigorous and time-consuming procedure, allowing regulation of metabolic substrates and insulin levels and providing excellent image quality in most patients,[46] especially in those with non–insulin-dependent diabetes mellitus (protocol 4A). A shorter IV glucose/insulin-loading procedure (30 minutes) has also been used with some success[47] (protocol 4B).
3. **Acipimox.** Acipimox is not currently available in the United States but has been used successfully in Europe instead of glucose loading. Acipimox is a nicotinic acid derivative inhibiting peripheral lipolysis, reducing plasma free fatty acid levels, and indirectly stimulating myocardial glucose utilization.[48,49]

Two Sample IV Protocols

4. **Protocol A.** A sample protocol for IV glucose loading is presented. This protocol is based on one in use at Vanderbilt University Medical Center, Nashville, Tenn, and is adapted from Martin et al.[48]

4.1. IV glucose/insulin loading for nondiabetic patients and fasting BG is less than 110 mg/dL:

4.1.1. Prepare dextrose/insulin solution: 15 U of regular insulin in 500 mL of 20% dextrose in a glass bottle. The initial 50 mL is discarded through the plastic IV tubing (no filter) to decrease adsorption of the insulin to the tubing.
4.1.2. Prime the patient with 5 U of regular insulin and 50 mL of 20% dextrose (10 g) IV bolus.
4.1.3. Infuse dextrose/insulin solution at a rate of 3 $mL \cdot kg^{-1} \cdot h^{-1}$ for 60 minutes (corresponding to an insulin infusion of 1.5 $mU \cdot kg^{-1} \cdot min^{-1}$ and a glucose infusion of 10 $mg \cdot kg^{-1} \cdot min^{-1}$). Monitor BG every 10 minutes (goal BG, 100-200 mg/dL).
4.1.4. If BG at 20 minutes is 100 to 200 mg/dL (preferably <150 mg/dL), administer FDG intravenously.
4.1.5. If BG is greater than 200 mg/dL, administer small IV boluses of 4 to 8 U of regular insulin until BG decreases to less than 200 mg/dL. Administer FDG intravenously.
4.1.6. Stop dextrose/insulin infusion at 60 minutes, and start 20% dextrose at 2 to 3 $mL \cdot kg^{-1} \cdot h^{-1}$.
4.1.7. During image acquisition, continue infusion of 20% dextrose at 2 to 3 $mL \cdot kg^{-1} \cdot h^{-1}$.
4.1.8. At completion of the acquisition of the images, discontinue infusion, give a snack to the patient, and advise him or her regarding the risk of late hypoglycemia.
4.1.9. **ALERT:** (1) If BG is greater than 400 mg/dL, call the nuclear physician immediately. (2) If BG is less than 55 mg/dL or if the patient develops symptoms of hypoglycemia with BG less than 75 mg/dL, discontinue dextrose/insulin infusion, administer one amp of 50% dextrose intravenously, and call the nuclear physician.

4.2. IV glucose/insulin loading for diabetic patients or fasting BG greater than 110 mg/dL:

4.2.1. Prepare insulin solution: 100 U of regular insulin in 500 mL of normal saline solution in a glass bottle. The initial 50 mL is discarded

through the plastic IV tubing (no filter) to decrease adsorption of the insulin to the tubing.

4.2.2. Prime patient with regular insulin:

4.2.2.1. If fasting BG is greater than 140 mg/dL, prime the patient with 10 U of regular insulin IV bolus.

4.2.2.2. If fasting BG is less than 140 mg/dL, prime the patient with 6 U of regular insulin IV bolus.

4.2.3. Infuse insulin solution at a rate of 1.2 $mL \cdot kg^{-1} \cdot h^{-1}$ for 60 minutes (corresponding to an insulin infusion of 4 $mU \cdot kg^{-1} \cdot min^{-1}$) or for the entire study (to calculate the regional glucose utilization rate).

4.2.4. After 8 to 10 minutes or when BG is less than 140 mg/dL, start 20% dextrose infusion at 1.8 $mL \cdot kg^{-1} \cdot h^{-1}$ (corresponding to a dextrose infusion of 6 $mg \cdot kg^{-1} \cdot min^{-1}$).

4.2.5. Monitor BG every 5 to 10 minutes and adjust dextrose infusion rate to maintain BG at 80 to 140 mg/dL.

4.2.6. After 20 to 30 minutes of stable BG, administer FDG.

4.2.7. Maintain the IV infusion of insulin plus 20% dextrose for 30 to 40 minutes after FDG injection or until the end of the scan (to calculate rMGU [rate of glucose utilization]). Some centers confirm FDG uptake particularly in patients with diabetes before discontinuing the clamp.

4.2.8. At completion of the acquisition of the images, discontinue infusion, give a snack to the patient, and advise him or her regarding the risk of late hypoglycemia.

4.3. For lean patients with type 1 juvenile-onset diabetes mellitus, alter protocol 4.2 as follows:

4.3.1. If fasting BG is less than 140 mg/dL, inject 4 U of regular insulin and infuse insulin solution (prepared as in 4.2.1 above) at 0.3 $mL \cdot kg^{-1} \cdot h^{-1}$ (1 $mU \cdot kg^{-1} \cdot min^{-1}$).

4.3.2. After 8 to 10 minutes of infusion or when BG is less than 140 mg/dL, start 20% dextrose at 2.4 $mL \cdot kg^{-1} \cdot h^{-1}$ (8 $mg \cdot kg^{-1} \cdot min^{-1}$).

4.4. Some centers (Munich, Ottawa, and others) have also applied a front-loaded infusion.

4.4.1. About 6 hours after a light breakfast and their usual dose of insulin or oral hypoglycemic, all diabetic patients have a catheter inserted in one arm for glucose and insulin infusion, as well as a catheter in the opposite arm for BG measurement.

4.4.2. At time 0, the insulin infusion is started. Regular insulin is given at 4 times the final constant rate[50] for 4 minutes, then at 2 times the final constant rate for 3 minutes, and then at a constant rate for the remainder of the study.

4.4.3. If the BG is greater than 200 mg/dL, an additional bolus of insulin is given. An exogenous 20% glucose infusion is started at an initial rate of 0.25 $mg \cdot kg^{-1} \cdot min^{-1}$ and adjusted until steady state is achieved. The BG concentrations are measured every 5 minutes during the insulin clamp. The glucose infusion is adjusted according to the plasma glucose over the preceding 5 minutes.

5. **Protocol B.** A sample protocol for IV glucose loading is presented. Protocol B is based on the protocol in use at the Emory University–Crawford Long Memorial Hospital (Atlanta, Ga).[47] This protocol has been used in over 600 subjects (over one third of whom were diabetic), resulting in good-quality images in over 98% of studies.

5.1. If fasting BG is less than 125 mg/dL, give 50% dextrose in water (D-50-W), 25 g, intravenously. Hydrocortisone, 20 mg, should be added to the D-50-W to minimize the rather severe pain that can occur at the injection site with D-50-W. This is compatible and avoids the pain that limits patient cooperation. There is no negative effect on the quality of the FDG studies.

5.2. If fasting BG is between 125 and 225 mg/dL, give D-50-W, 13 g, intravenously.

5.3. If fasting BG is greater than 225 mg/dL, administer regular aqueous insulin as per the following formula: Regular aqueous insulin (dose units) = (BG − 50)/25.

5.4. After 30 to 60 minutes, if BG is less than 150 mg/dL, give FDG intravenously, but if BG is greater than 150 mg/dL, give more regular insulin, using the formula in 5.3 above, until BG is less than 150 mg/dL, before giving FDG. Giving FDG when BG is 150 to 200 mg/dL resulted in many poor-quality studies.

FDG cardiac PET acquisition parameters. Acquisition parameters for PET cardiac FDG imaging are itemized in Table 7 and its accompanying notes.

Most of the literature about viability and prediction of recovery after revascularization with PET is based on mismatch perfusion/metabolism (see Part 2 of these guidelines). N-13 ammonia and Rb-82 provide optimal perfusion images for comparison because the images are acquired with the same PET system and can be displayed with similar parameters as the FDG images. However, if these PET perfusion agents are not available, the FDG images can be interpreted in conjunction with SPECT perfusion images (see Part 2 below).

This comparison of PET to SPECT can be difficult

Table 7. FDG cardiac PET: Acquisition guidelines (for dedicated, multicrystal PET scanner)

Feature		Technique	For details, see note in text
Dose	5-15 mCi (185-555 MBq)	Standard	1
Image start time	45-60 min after injection (keep constant for repeat studies)		2
Image duration	10-30 min (depending on count rate and dose)		3
Acquisition modes	2D	Standard	4
	3D	Standard	4
	Static	Standard	4
	Dynamic	Optional	4
Total counts	Knowledge of machine performance characteristics (eg, noise-equivalent counts) is essential		5
Pixel size (reconstructed)	2-3 mm	Preferred	6
	4-5 mm	Acceptable	6
Attenuation correction	Measured attenuation correction: before or immediately after scan	Preferred	7
	Segmented attenuation correction	Acceptable	7
Reconstruction method	FBP or iterative expectation maximization (eg, OSEM)	Standard	8
Gating	ECG gating of myocardium	Standard	9
Patient positioning	Arms out	Preferred	10
	Arms in (not moving)	Optional	10

because of the absence or difference in the type of attenuation correction for SPECT, as well as the usual registration problems when comparing images on different instruments. Guidelines for SPECT perfusion imaging have been published previously[51] and are being updated concurrently. It should be noted that if Tl-201 or Tc-99m SPECT perfusion scanning has been performed, no waiting period is necessary (from an instrumentation point of view) before the PET scanning is begun if the 2D acquisition mode is used. The photons from Tl-201 and Tc-99m do not interfere. Caution needs to be used with 3D imaging, since the Tc-99m activity can increase dead time and thus decrease the "true" counts from the FDG. On the other hand, after administration of a PET tracer, it is usually necessary to wait at least 15 or more half-lives (depending on dose) before a low-energy (eg, Tl-201 or Tc-99m) scan is performed. This is because the 511-keV photons from the PET tracers easily penetrate the collimators most commonly used for Tl-201 or Tc-99m imaging.

Notes for Table 7: Image Acquisition

1. Dose. Typically, 5 to 15 mCi is injected in a peripheral vein (see counts requirements below). Injection speed is not critical (bolus to 2 minutes). To reduce patient dose to the bladder, patients should be encouraged to void frequently for 3 to 4 hours after the study.
2. Wait a minimum of 45 minutes before starting the static scan. Uptake may continue to increase and blood pool to decrease as time progresses, even after 45 minutes. Longer than 90 minutes may give better blood pool clearance and uptake, when necessary (eg, diabetic or high-BG subjects), but could result in reduced count rate. If a follow-up FDG PET study is envisioned, it is important to duplicate the timing of the scan. Because FDG uptake is time-dependent (ie, it is possible that uptake may continue beyond 60 minutes), comparing two scans acquired at different post-injection acquisition times can be misleading.
3. Duration is typically 10 to 30 minutes. If acquired in 3D mode (ie, septa-out), compared with 2D mode with the same machine, a smaller dose is typically required to achieve the same total count rate, but the imaging time may or may not be reduced, as a result of count rate limitations and increased scatter. In some machines, beyond a certain dose, septa-out mode (3D) will actually produce poorer-quality images for the same dose and imaging time than septa-in (2D) mode. For this reason, it is critical to have fully characterized the performance of the system.

4. Static versus dynamic acquisition: Static acquisition produces images that allow relative quantification of FDG uptake on a regional basis. Such images (along with perfusion images) are the standard basis for making viability determinations.[1-3] However, there is one form of dynamic imaging that has a significant practical advantage. Consider what is normally the 10- to 30-minute duration static scan, begun around 60 minutes after injection. It is clinically desirable to acquire these data as a 3-frame or greater dynamic data set. If the patient should move during the end of the study, one can then utilize only those dynamic frames with no motion (summing them together to make one static image). This is easily implemented and takes almost no additional operator time. A more elaborate dynamic acquisition may optionally be used when FDG kinetic analysis over the entire uptake period is to be performed (eg, compartmental analysis or Patlak analysis). Kinetic analysis permits absolute quantification of the rate of FDG utilization. Performing and interpreting such kinetic analyses[52] can be complex and require experience with kinetic modeling.
5. The counts per slice necessary to yield adequate-quality images will vary from institution to institution depending on, among other things, scatter and randoms corrections, as well as the amount of smoothing that is done. If one tries to achieve on the order of 7 mm full width at half maximum (FWHM) in-plane resolution and has 10% to 15% scatter (National Electrical Manufacturers Association), then a typical good-quality study in 2D mode might have on the order of 50,000 true counts per millimeter of transaxial distance over the region of the heart (eg, for a 4.25-mm slice separation, the counts would be 50,000 $\times$ 4.25 = 250,000 counts per slice). These numbers are very approximate and may differ from one scanner type to the next. With a 10-mCi injected dose, these total counts could be achieved in 20 to 30 minutes depending on system sensitivity. If one is willing to accept a lower resolution (eg, more smoothing) or more noise, imaging time can be reduced. Low uptake and high blood pool activity situations (eg, diabetes or high glucose levels) may require longer imaging time and/or (preferably) later imaging times. Since 3D scanners have greater scatter, they usually require more counts than a 2D scanner to achieve the same noise level.
6. It is recommended that 2 to 3 mm per pixel be used. A "rule of thumb" in nuclear medicine physics is that one needs at least 3 pixels for every FWHM of resolution in the image. For example, if the data are reconstructed to 8-mm FWHM, then one needs roughly 8 mm/3 = 2.7 mm/pixel. Many institutions achieve a 3-mm sampling rate or better with a 256 $\times$ 256 array over the entire field of view of the camera. Other institutions choose to use a 128 $\times$ 128 array over a limited field of view (eg, 25-35 cm diameter) centered over the heart, in which case, 2 to 3 mm/pixel is easy to achieve (cutting out extraneous structures in the field of view) even with a 128 $\times$ 128 array. Either method is acceptable to achieve the desired 2 to 3 mm/pixel. Greater than 3 mm/pixel may be acceptable for older PET cameras with resolution worse than 1 cm.
7. Since attenuation correction is a far more severe problem in coincidence imaging than in SPECT imaging[31]; it is essential that accurate attenuation correction be performed. Segmented attenuation correction schemes may give errors for those slices that contain a mixture of lung and liver tissue adjacent to the heart. Similarly, the optimal CT-based attenuation correction to be used to image the heart for viability imaging will depend on the results of future research. Experience at several centers has shown that a slow CT acquisition, lasting 10 to 60 seconds during free breathing, at a low CT tube current, helps sample the average attenuation map, corresponding to the emission map.
8. FBP versus iterative reconstruction method: FBP is the standard method used for reconstruction. FBP images are subject to streak artifacts, especially when too short a transmission scan is used for attenuation correction (or when the subject is obese or large). This can affect visual analysis but usually does not adversely affect quantitative analysis with regions of interest (the streaks tend to average out properly over typical volumes of interest). Iterative methods (eg, the method of OSEM) have been adopted in other FDG imaging situations (eg, oncology), yielding images with better noise properties. Although high-uptake structures, such as the heart, may not improve their noise characteristics with OSEM, the surrounding lower-uptake structures do improve, and streak artifacts are nearly eliminated, thus greatly improving the visual appearance of the image. However, low-uptake areas (such as myocardial defects and the LV cavity at late times) may have slightly (artificially) elevated activity levels unless sufficient iterations are performed. It is recommended that one thoroughly characterize the PET machine and its reconstruction algorithm's behavior with a realistic cardiac phantom.
9. Usually, FDG PET counts are sufficiently large to yield a high-quality ventricular motion study (typically 8-16 time points), in a manner similar to SPECT gated perfusion studies (but at higher spatial

resolution). Given that ventricular contraction and thickening are often clinically useful for assessing viability, gating should be performed when possible. It is important that the gating software does not adversely affect the ungated images (eg, by loss of counts as a result of beat length rejection). Monitoring the length and number of the accepted beats is highly desirable.

10. Ideally, the patient should be positioned supine, with the arms out of the camera field of view. This can be tolerated by nearly all patients, provided some care is given to support of the arms or by use of an overhead bar to hold onto. There are, however, cases in which "arms-out" imaging is not possible (eg, in patients with severe arthritis), and imaging must be performed with the arms at the side. In this case the transmission scan time may have to be increased, and it is of critical importance that the arms not move between transmission and emission, or artifacts will result. In patients undergoing PET/CT imaging, arms in (down) the field of view may result in beam-hardening artifacts on the CT-based transmission scan, which usually lead to streak artifact of the corrected emission scans.

PART 2: INTERPRETATION AND REPORTING

A. General Comments

The purpose of evaluating myocardial perfusion during stress testing and at rest is to determine whether there is evidence of myocardial ischemia and/or infarction in those patients suspected of having CAD, as well as to determine the extent and severity of coronary disease and any dysfunction in both patients with known coronary disease and those with suspected coronary disease. The goals of diagnosing CAD are to direct specific therapy to alleviate symptoms of ischemia, to initiate appropriate steps to modify its risk factors, to retard its progression, and to improve patient outcomes. The diagnosis of CAD is also important in the selection of patients who need to be studied with invasive diagnostic methods (eg, coronary angiography), those with a high cardiac risk, those with a high need to know, and those with symptoms refractory to medical therapy. Evaluation of the severity of disease is critically important in the selection of those patients, in whom extensive and/or severe disease suggests that invasive interventional therapy is warranted by the possibility of improving clinical outcomes. Finally, myocardial perfusion imaging can be used for assessing the efficacy of medical or surgical treatment.

Myocardial perfusion imaging with PET can be accomplished with the flow tracers Rb-82 or N-13 ammonia, at rest and during pharmacologic or exercise stress. Normal myocardial perfusion obtained during adequate stress implies absence of significant CAD. Stress-induced regional myocardial perfusion abnormalities or inadequate augmentation in perfusion with stress implies epicardial CAD or possibly small-vessel disease. Impaired regional myocardial perfusion during both stress and rest suggests the presence of an irreversible myocardial injury.

Both N-13 ammonia and, particularly because of its short half-life, Rb-82 can be used sequentially with non-traditional maneuvers as well as traditional stress testing to identify and localize myocardial areas with ischemia and coronary dysfunction. This includes handgrip, cold-pressor testing, mental stress, nitroglycerin drip, and intra-aortic balloon pump. These applications are still evolving and in the process of clinical evaluation.

Myocardial metabolism imaging with PET serves to identify persistent metabolic activity in dysfunctional and hypoperfused myocardial regions. It is accomplished with F-18 FDG as a tracer of exogenous glucose utilization. The regional myocardial concentrations of this tracer are compared with the regional distribution of myocardial perfusion: Regional increases in FDG uptake relative to regional myocardial blood flow (perfusion-metabolism mismatch) signify myocardial viability—that is, reversibility of contractile dysfunction if regional blood flow is improved. In contrast, a regional reduction in FDG uptake in proportion to regional reductions in myocardial perfusion (perfusion-metabolism match) signifies irreversibility of contractile dysfunction.

The following guidelines for interpretation and reporting of PET myocardial perfusion and metabolism images assume that the studies were performed and processed in accordance with the guidelines as described in Part 1. In instances where myocardial FDG uptake was imaged with SPECT, as is also outlined in Part 1 of these guidelines, the interpretation of the metabolic images must then consider technical and methodologic aspects unique to positron imaging with SPECT and methodologic differences between PET and SPECT. This also pertains to situations where metabolism has been imaged with PET and perfusion with SPECT. Special consideration must also be given to studies when only images of myocardial metabolism but not of myocardial perfusion have been acquired.

B. Display of Perfusion and Metabolism

i. **Recommended medium for display.** According to the previously established guidelines for myocardial SPECT imaging, it is strongly recommended for the reading physician to use the computer monitor rather

than film hard copies for interpretation of myocardial perfusion and metabolism images. A linear gray scale, a monochromatic color scale, or a multicolor scale can be used as the type of display, depending on user experience and preference.

ii. **Conventional slice display of PET perfusion and metabolism images.** Recommendations for display of PET perfusion rest-stress and/or perfusion-metabolism images are consistent with those listed in previous guidelines for SPECT myocardial rest-stress perfusion imaging. It is necessary to examine the transaxial, coronal, and sagittal views—that is, the not-yet-reoriented images for assessing the alignment of the emission images acquired during different conditions, rest and stress perfusion, and metabolism, as well as the transmission images. Fused transmission and emission images are preferred. If the images are not aligned because of patient or cardiac motion, this may cause serious image artifacts, especially when only one set of attenuation correction images has been applied to all emission images for attenuation correction.

For interpretation, the reoriented images should be displayed as follows:

1. A short-axis view, by slicing perpendicular to the long axis of the left ventricle from apex (left) to base (right).
2. A vertical long-axis view, by slicing vertically from septum (left) to lateral wall (right).
3. A horizontal long-axis view, by slicing from the inferior (left) to the anterior wall (right).

For interpretation and comparison of perfusion and metabolism images, slices of all data sets should be displayed aligned and adjacent to each other.

Software routines are available for handling of image data from different camera systems and for a combined display of both SPECT and PET images. Combined assessment of perfusion and metabolism within a single PET session offers the advantage that, provided that the patient's position has not changed between the two acquisition periods, the ventricular long axis defined during image orientation can be copied from one image set to the second set so that matching of the perfusion with the metabolism images is optimized.

Normalization of the stress perfusion with resting perfusion images is commonly performed by using the maximal myocardial pixel value in each of the two or three image sets (or, for example, the average pixel value with the highest 5% of activity) of the perfusion images. Each perfusion study is then normalized to its own maximum.

The metabolism images are normalized to the counts in the same myocardial region on the resting perfusion images (eg, with the highest count rates that were obtained on the perfusion study).[53,54] Because glucose metabolism may be enhanced in regions of normal perfusion, as might occur in postischemic stunning, this normalization approach allows for more accurate identification and interpretation of perfusion-metabolism mismatch or match patterns.

iii. **Three-dimensional display.** Display of the reconstructed image data in a 3D static or cine mode is optional and may be convenient for morphologic correlation with magnetic resonance or angiographic images, if suitable software is available. Currently, however, an advantage of 3D over conventional 2D displays with regard to accuracy of PET image interpretation remains to be demonstrated.

iv. **Polar maps.** Polar maps of PET rest and stress perfusion images and FDG metabolic images are based on a circumferential profile of the corresponding short-axis slices, in the same way as polar maps of SPECT myocardial perfusion images (see concurrently updated guidelines on myocardial SPECT perfusion images), and are commonly used for visual and semiquantitative assessment. These derivative polar maps, while useful, should not be considered a substitute for the examination of the standard short-axis and long-axis cardiac tomographic slices.

C. Evaluation of Images for Technical Sources of Errors

Each laboratory should perform the daily QC recommended by the manufacturer of the PET camera to be certain that the detector blocks are working appropriately. Normalization of the detectors (usually monthly) should also be performed according to the manufacturer's recommendations.

When FDG PET metabolic images are evaluated with SPECT perfusion images, examination of the SPECT images for artifacts should be performed as recommended in the previously developed guidelines for SPECT myocardial perfusion imaging.

i. **Patient motion.** PET images are typically generated with nonmoving circular arrays of scintillation detectors that acquire all projection data. In contrast to SPECT imaging with rotating gamma cameras, in which patient motion leads to a typical misalignment between adjacent projection images and can be identified by viewing a projection movie, movement during static PET imaging affects all projections and is therefore more difficult to identify. Blurring of contours results from substantial patient motion; it is most easily confirmed by viewing non-reoriented transaxial images or the sinograms. Algorithms for motion correction during static PET imaging have not become available. While repeat imaging with FDG is feasible, and repeat imaging with

rest Rb-82 is easily achieved with a second injection and acquisition, repeat imaging with stress is usually not an option. Therefore attention to patient motion during image acquisition is essential for avoidance of motion artifacts. Patient positioning before and immediately after image acquisition should be carefully evaluated (eg, by checking the alignment of the camera's positioning laser beams with ink markers on the patient's skin). Acquisition of a brief scan or scout image after injection of a small dose, usually one third of the standard dose of Rb-82 or N-13 ammonia, may facilitate accurate patient positioning. With PET/CT systems, a CT scout scan (10 mA) is routinely used for accurate patient positioning. In instances of patient discomfort and likely patient motion, especially during longer image acquisition times as with FDG, possible approaches to reducing adverse effects of motion include acquisition of a series of 3 to 4 sequential image frames instead of a single static image of longer duration. If the quality of one of the serially acquired frames is compromised by motion, then that frame can be rejected and only frames that are of acceptable quality and are free of motion artifacts are summed for the final image analysis.

ii. **Attenuation correction.** Correction of the emission images for photon attenuation is critical for cardiac PET imaging. Positron-emitting tracers are more sensitive than single photons to attenuation artifacts. Both simultaneously emitted photons must be detected by the coincidence detection systems. As each of the two photons is susceptible to tissue attenuation, attenuation artifacts are generally greater. Therefore only attenuation-corrected images should be used for clinical interpretation. Potential sources of errors include misalignment between emission and transmission data resulting from patient motion. Misalignments of 1.5 to 2 cm, for example, can lead to as much as a 30% change in the observed regional myocardial radioactivity.[55,56]

Vertical and transaxial displacement of the heart can occur even in the absence of movement of the chest, perhaps because of a change in the pattern of breathing, which may occur during pharmacologic stress. It is analogous to the "upward creep" seen in SPECT imaging. This can result in anterior or anterolateral defects (usually resulting from under-correction due to the lower attenuation coefficient of the overlapping lung tissue) or inferior "hot spots" (usually resulting from over-correction due to the higher attenuation coefficients of the overlapping subdiaphragmatic tissues). Inspection of fused emission-transmission images for possible misalignment is essential because the resulting artifacts would greatly affect image interpretation.

Identification of vertical and lateral displacements that result in misalignment between the emission and transmission images is relatively straightforward upon careful inspection of the fused emission-transmission data sets. Fused images should be inspected in the axial (lateral displacement) as well as the coronal (vertical displacement) and sagittal (vertical displacement) slices. Alternatively, displacement can be detected on transaxial images by counting the number of pixels by which the cardiac image is displaced between resting and stress transaxial acquisitions.

The degree of co-registration of transmission and emission images should be carefully examined using the fusion software available on integrated PET-CT systems to assess the reliability of images with attenuation correction. If there is patient motion and the cardiac silhouette does not superimpose perfectly on the transmission and emission images, the images without attenuation correction need to be examined as well. When the transmission maps are acquired using CT, the incidental findings in the portion of the chest in the field of view should be reported when relevant to patient care.

In general, vertical misalignment might be easier to resolve by off-setting the alignment between the emission and transmission scans, but this option is not generally available.

iii. **Reconstruction artifacts.** Image artifacts may occur if extracardiac activity is present adjacent to the myocardium. For example, intense focal activity in the liver or the gastrointestinal tract may cause a reconstruction artifact with artifactually low count rates in adjacent myocardium. A method to correct for such artifacts is currently not available, but such artifacts are less prominent when iterative reconstruction is used instead of the standard FBP techniques. Streak artifacts may result from nonuniformity due to malfunctioning blocks of detector crystal. Streak artifacts result from problems with CT transmission images, such as insufficient x-ray tube intensity in obese individuals, breathing mismatch, truncation, and beam hardening resulting from bone (arms down) or metal adjacent to the heart (pacemakers and internal defibrillators).

iv. **Image count statistics.** The final count density of PET images is influenced by additional factors such as body weight and build, radionuclide dose, scanner performance, acquisition time, and in the case of metabolic imaging, the dietary and hormonal state. Image count density directly affects the diagnostic quality and reliability of the study.

D. Image Analysis and Interpretation of Perfusion Images

The rest and stress perfusion images, if obtained, and FDG images should be interpreted initially without clinical information in order to minimize any bias in study interpretation. All relevant clinical data should be

reviewed after a preliminary impression is formed. The following sections address first the interpretation of the perfusion images and then the interpretation of the metabolism images, if available. The latter section then continues by describing the correlation of findings on the metabolism image to those on the perfusion images.

i. **Left and right ventricular size.** The reader should note whether there is an enlargement of the right or left ventricle at rest or whether there is transient stress-related LV dilation if such images were obtained. Ventricular enlargement seen on the stress and rest perfusion images, as well as on the FDG images, generally indicates left, right, or bi-ventricular dysfunction. Transient stress-related LV dilation usually reflects extensive CAD. LV and right ventricular (RV) sizes as well as any changes associated with stress are typically described qualitatively. It is important to be sure that Rb-82 blood pool activity has cleared from the LV cavity, in order to be sure that there is not an artificial underestimation of LV cavity at rest. A number of commercially developed software packages originally developed for SPECT have the ability to quantitate mean LV volumes and end-diastolic and end-systolic volumes for gated PET images, but not all such packages have been validated for all PET instruments, and they should be used with caution.

ii. **Lung uptake.** Increased tracer activity in the lungs should be reported qualitatively. Increased lung uptake on the perfusion images, particularly when severe, may reflect severe LV dysfunction with increased LV filling pressures. Mild to moderate lung uptake may occasionally be seen in patients with chronic pulmonary disease and in smokers.

iii. **RV uptake.** The degree of RV tracer uptake should also be noted. It is usually described qualitatively. Increases may be seen in the presence of pulmonary hypertension with or without significant RV hypertrophy. RV hypertrophy may alter the shape of the left ventricle and produce both "hot" and "cold" areas in the septum and adjacent LV areas. However, no definite criteria have been established for defining abnormally increased RV tracer uptake.

iv. **Blood pool activity.** Increased blood pool activity is usually a sign of relatively poor myocardial uptake of the flow tracer, insufficient time for tracer uptake into the myocardium, or diminished clearance from blood. A major cause of increased blood pool activity, especially for perfusion imaging with Rb-82, is impairment of cardiac systolic function that prolongs the circulation time. This is especially relevant when only static images are acquired, because vasodilators typically increase cardiac output and shorten the circulation time. Increased blood pool activity may be seen if the acquisition of images begins prior to 5 to 7 minutes after N-13 ammonia administration or prior to 70 to 170 seconds after Rb-82 administration, especially in patients with a history of congestive heart failure and poor LV function. If Rb-82 perfusion images are acquired serially, an appropriate starting point, after blood pool activity has cleared sufficiently, can be chosen after the acquisition for summing the myocardial tracer uptake images. Judicious adjustment of display threshold and contrast settings can help offset this problem.

v. **Noncardiac findings.** The tomographic images should be carefully examined for uptake of the radiotracer in organs other than the myocardium, particularly in the lungs and the mediastinum. Extracardiac uptake of a flow tracer may be of clinical significance, as it may be associated with malignancy and/or an inflammatory process. The 3D maximum intensity projection display, a method of displaying acquired PET images as a rotating 3D display, can be particularly helpful in this regard. When using PET/CT systems, review of the low-resolution CT-based transmission scans can be useful to delineate potentially important ancillary findings (pleural and pericardial effusion, coronary and/or aortic calcification, lung mass, and so on).

vi. **Perfusion defect location.** Myocardial perfusion defects should be identified through careful visual analysis of the reoriented myocardial slices. Perfusion defects should be characterized by extent and location relative to the specific myocardial territory, such as the anterior, lateral, inferior, septal, and/or apical walls. Standardized nomenclature should be used, according to previously published guidelines relating to SPECT perfusion imaging. RV defects due to scarring and ischemia should be noted.

vii. **Perfusion defect severity and extent: Qualitative.** Defect extent may be qualitatively described as small (5% to 10% of the left ventricle), medium (15% to 20% of the left ventricle), or large (>20% of the left ventricle). Alternatively, defect extent may also be estimated by describing the segments involved, such as "mid and distal" or "extending from base to apex," in a particular LV area. Defect severity is typically expressed qualitatively as mild, moderate, or severe. Severe defects may be considered as those having a tracer concentration equal or similar to background activity, and moderate defects are considered definitely abnormal but less severe. Mild defects are those with a subtle but definite reduction in regional myocardial tracer concentration that are, however, of uncertain clinical significance. Perfusion defects that remain unchanged in extent and severity between the stress and rest images are typically categorized as fixed or nonreversible. In contrast, defects that decrease in extent, in severity, or both from stress to rest are categorized as reversible, in which case a

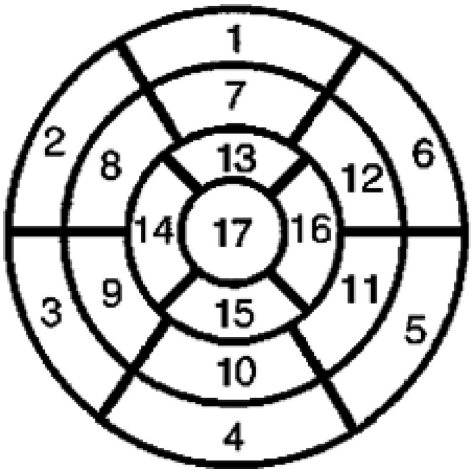

Figure 1. Seventeen-segment nomenclature. Segments 1, 7, and 13 represent the basal (*1*), mid (*7*), and apical (*13*) anterior segments. Segments 4, 10, and 15 represent the basal (*4*), mid (*10*), and apical (*15*) inferior segments. The septum contains 5 segments: basal anteroseptal (*2*), basal inferoseptal (*3*), mid anteroseptal (*8*), mid inferoseptal (*9*), and apical septal (*14*). The lateral wall is divided into the basal anterolateral (*6*), basal inferolateral (*5*), mid anterolateral (*12*), mid inferolateral (*11*), and apical lateral (*16*). The long-axis segment is called the apex (*17*). (Reprinted with permission from American Society of Nuclear Cardiology. Imaging guidelines for nuclear cardiology procedures, part 2. J Nucl Cardiol 1999;6:G47-84.)

description of the degree of defect reversibility is required (see below).

viii. **Perfusion defect severity and extent: Semiquantitative.** In addition to the qualitative assessment of perfusion defects, the reader may also apply semiquantitative approaches based on a validated segmental scoring system. This approach standardizes the visual interpretation of scans, reduces the likelihood of overlooking clinically significant defects, and provides a semiquantitative index that is applicable to diagnostic and prognostic assessments.

A 17-segment model for semiquantitative visual analysis is usually employed. The model is based on three short-axis slices (apical, mid, and basal) to represent most of the left ventricle and one vertical long-axis slice to better represent the LV apex. The basal and mid short-axis slices are divided into 6 segments. The apical short-axis slice is divided into 4 segments. A single apical segment is taken from the vertical long-axis slice. Each segment has a specific name (Figure 1).

The extent of stress and rest perfusion abnormalities, as well as an estimate of the extent of scarring and ischemia, can be performed by counting the number of segments.

Myocardial segments may be assigned to coronary artery territories. Caution should be exercised because the coronary anatomy varies widely among patients. For example, it is not at all uncommon to find segments 9, 10, and 15 of the 17-segment model involved in left anterior descending artery disease. Similarly, segments 5 and 11 of the model may be affected by disease of the right coronary artery.

Table 8. Semiquantitative scoring system of defect severity and extent

Grade	Interpretation	Score
Normal counts	Normal perfusion	0
Mild reduction in counts	Not definitely abnormal	1
Moderate reduction in counts	Definitely abnormal	2
Severe reduction in counts	Definitely abnormal	3
Absent counts	Definitely abnormal	4

Semiquantitative scoring system. The scoring system provides a reproducible semiquantitative assessment of defect severity and extent (Table 8). A consistent approach to defining defect severity and extent is clinically important because each of the two variables contains independent prognostic power. Furthermore, semiquantitative scoring can be used to more reproducibly and objectively designate each segment as normal or abnormal. Points are assigned to each segment in direct proportion to the observed count density of the segment.

In addition to individual scores, calculation of summed scores is recommended, in which the summed stress score is the sum of the stress scores of all segments, the summed rest score is the sum of the resting scores or redistribution scores of all segments, and the summed difference score is the difference between the summed stress and summed rest (redistribution) scores and serves as a measure of reversibility.

Before scoring, it is necessary for the interpreting physician to be familiar with the normal regional variation in count distribution of myocardial perfusion PET. For example, retention of N-13 ammonia in the lateral and basal inferolateral wall of the left ventricle may be diminished in normal subjects. In severity, this normal variant reduction may be mild to moderate and should be considered when analyzing rest or stress N-13 ammonia images. No such regional variation in tracer uptake has been reported for Rb-82, except for a mild reduction in the apex and base, consistent with the known thinning of the LV myocardium in these locations.

ix. **Perfusion defect severity and extent: Quantitative.** Quantitative analysis aids in supplementing the visual interpretation. Most quantitative analyses require display of the tomographic slices in a polar map

format that provides an easily comprehensible representation of the extent, severity, and reversibility of perfusion abnormalities.[53,57,58] The patient's polar map is compared with a reference polar map derived from normal individuals. Because of the differences in tracer distributions throughout the LV myocardium, the use of separate databases for N-13 ammonia and Rb-82 is recommended. Each camera system and acquisition protocol should have its own "normal" file. The quantitative estimates should appropriately sample all segments of the left ventricle. The quantitative analysis system should be validated by appropriate studies published in peer-reviewed journals. Such systems typically describe the extent of a perfusion defect in terms of percentage of LV myocardium. These analysis systems further offer an index of the average severity of a perfusion defect.

Myocardial blood flow in absolute units of milliliters of blood per minute per grams of myocardium. A quantitative estimate of myocardial blood flow can complement the visual interpretation. Estimating myocardial blood flow in absolute units requires acquisition of dynamic imaging data sets.[7,59-61] Regions of interest are placed on the LV myocardium and the LV blood pool and are copied to all serially acquired images for generation of myocardial tissue and blood pool time-activity curves. The time-activity curves are corrected for activity spillover from the blood pool to the myocardium and for radioactive decay. They are then fitted with a validated tracer kinetic model, and estimates of myocardial blood flow in milliliters of blood per minute per grams of myocardium are obtained. Software programs are also available for generating parametric polar maps that display regional myocardial blood flows in absolute units.[6,62]

Quantitative blood flow approaches offer an objective interpretation that is inherently more reproducible than visual analysis. Absolute quantitation may aid in assessing the physiologic significance of known coronary stenoses, especially when of intermediate severity. Both relative quantitation and absolute quantitation are particularly useful in describing changes between two studies in the same patient. In addition, quantitative measurements of myocardial blood flow may aid in the detection of balanced reductions in myocardial blood flow due to multivessel CAD and, thus, may be useful for assessing the true extent of disease. Quantitative assessment of myocardial blood flow at rest and stress can help detect an inadequate response to stress, resulting in decreased sensitivity for regional epicardial CAD, or can help detect the presence of diffuse small-vessel disease.

x. **Reversibility of flow defects.** The degree of defect reversibility may be categorized as complete or partial. It is important to note the Rb-82 clearance from the LV blood pool, because if there is excess Rb-82 at rest, it can scatter into the subendocardial defect to make the resting scan appear artificially normal and the defect appear artificially reversible. Adjustment of display settings and contrast can partly help to adjust for this discrepancy. Complete reversibility is present when the tracer activity within the defect returns to a level comparable to the surrounding normal myocardium. Because the term *partial* often includes segments with a wide range of reversibility, it is recommended that the terms *moderate* or *significant but not complete* be used instead to describe the degree of change in tracer activity from stress to rest. The semiquantitative scoring system may be used to define significant reversibility as improvement of 2 grades or more or as improvement to a score of 1. The degree of reversibility on a quantitative polar map will depend on the particular software routine in use and the normal reference databases used in that program, but it is more objective.

xi. **Gated myocardial perfusion PET images.** ECG gating of the rest and peak stress images can provide additional information regarding changes in LV function and volumes that may be useful in identifying 3-vessel CAD with or without left main disease, which may be underestimated on the review of the perfusion images. Unlike ECG gating of the post-stress SPECT images, PET acquisitions take place during peak stress, especially when using ultra–short-lived tracers like Rb-82 (acquisitions are shorter than those for N-13 ammonia and, thus, more likely to occur while the patient is in peak pharmacologic stress). Recent data suggest that estimates of LVEF during peak stress and their change from baseline correlate with the magnitude of ischemia on the perfusion images and are useful measures to identify balanced ischemia resulting from extensive obstructive CAD.[63]

E. Interpretation of FDG Metabolism Images

i. **Noncardiopulmonary findings.** The tomographic images should be carefully examined for uptake of FDG in organs other than the heart, particularly the lungs and mediastinum. Extracardiac uptake of FDG may be of clinical significance as it may represent malignancy and/or inflammatory disease. FDG may be taken up in atherosclerotic plaques visible in the aorta and other larger arteries. The 3D rotating maximum intensity projection display can be particularly helpful. If focal areas of FDG uptake are visualized outside of the heart, a whole-body PET acquisition may be useful for defining areas of abnormality more completely. One should note, however, that whole-body, non-fasting, glucose-loaded and insulin-supplemented FDG images may demonstrate different distribution than in the fasting state, featuring

higher uptake in skeletal muscles and possibly lower uptake in tumors.

ii. **Blood pool activity.** Increased blood pool activity is usually a sign of diminished clearance of radiotracer from blood into tissue and into the myocardium. It is important to note this finding while the patient is still in the scanner, while it is easiest to take corrective measures. This increase in blood pool activity may be caused by the following:

1. Inadequate patient preparation with high free fatty acid and low insulin plasma levels, as occur, for example, after fasting and without glucose loading, so that tracer clearance from blood is delayed.
2. States of insulin resistance (insulin resistance, impaired glucose tolerance, and type 2 diabetes mellitus).
3. Type 1 diabetes mellitus.
4. Elevated plasma glucose concentrations with an increase in the distribution volume for FDG.
5. Insufficient time for clearance of tracer from blood into tissue before image acquisition.

High blood pool activity reduces the image contrast and, thus, the diagnostic quality of the images. Blood pool activity frequently declines with time so that relative myocardial FDG uptake increases. Repeat imaging after an additional 30 to 60 minutes may improve the myocardium–to–blood pool contrast but at the expense of lower count densities because of radioactivity decay. The image quality can be improved and controlled by careful patient preparation as detailed in Part 1 of these guidelines. It is also possible to accelerate the clearance of FDG from blood and its uptake into myocardium by IV administration of regular short-acting insulin while carefully monitoring BG levels to avoid hypoglycemia.[44,46]

iii. **Myocardial FDG uptake: Distribution and extent of viability—Qualitative.** After inspection of the transaxial myocardial views for movement artifacts, myocardial metabolism should first be evaluated through visual analysis of the reoriented myocardial image slices. An initial determination of the degree of FDG uptake in the "best"-perfused myocardial territory aids in recognizing whether images were acquired in the fasting state or after a glucose load. In the fasting state, normal (ie, "best"-perfused) myocardium will show minimal or low FDG uptake because of its preferential fatty acid uptake.[42,64,65] This "hot spot" imaging condition may be difficult to interpret because the image normalization process further augments the regional FDG accumulation, which may prompt an overestimation of the actual degree of a perfusion metabolism mismatch and thus lead to an overestimation of myocardial viability. On images obtained after glucose loading, either by mouth or intravenously, the increase in plasma glucose concentrations prompts secretion of insulin and thereby shifts the myocardium's substrate utilization from free fatty acid to glucose. This shift in substrate utilization is associated with increased FDG uptake both in normally perfused and in dysfunctional myocardium. Therefore, FDG uptake may be highest in the "best"-perfused myocardium. The extent and location of regional myocardial reductions in FDG uptake should be analyzed and described analogous to the qualitative description of perfusion defect severity and extent as described above.

Table 9. Semiquantitative scoring system of distribution and extent of viability

Grade	Interpretation*	Score
Highest counts	Normal or ischemia	0
Mildly lower counts		1
Moderately lower counts		2
Severely reduced counts		3
Absent counts		4

*This scoring system applies to studies performed in the glucose-loaded state and high FDG uptake in normal ("best" perfused) myocardium. The same scoring system may also be used for studies with lower FDG uptake in normal myocardium; the description of the findings should then, however, indicate the segments that are considered normal as judged from the perfusion images.

iv. **Metabolism: Distribution and extent of viability—Semiquantitative.** Analogous to the semiquantitative evaluation of the perfusion images, the use of a scoring system provides a reproducible semiquantitative assessment of the extent and severity of regional alterations in FDG uptake. Such semiquantitative scoring can be used to more reproducibly and objectively designate segments as metabolically viable or nonviable. Scores are assigned to each segment in direct proportion to the observed count density of the segment (Table 9).

Before scoring, it is necessary for the interpreting physician to be familiar with the normal regional variation in count distribution of myocardial metabolism, as well as with the dietary condition of the patient at the time of FDG imaging. Importantly, FDG concentrations in the normal myocardium may be increased in the lateral and posterolateral wall.[42,66] This normal variant is observed especially when metabolism is imaged in the fasting state and FDG uptake is low in the interventricular septum and the anterior wall but increased in the lateral and posterolateral wall.

The interpretation should include a description of the probability for the potential for improvement in regional contractile function and in LVEF. The potential for a post-revascularization improvement in contractile function is low for perfusion-metabolism matches, even if the regional reductions in perfusion and in FDG uptake are only mild or moderate. Conversely, the potential for improve-

ments in regional contractile dysfunction is high if perfusion is normal, if both perfusion and FDG uptake are normal, or if FDG uptake is significantly greater than regional perfusion (mismatch). Finally, the potential of a post-revascularization improvement in LVEF by at least 5 or more EF units is high if the mismatch affects 20% or more of the LV myocardium.[44,67,68]

NOTE: Comments by the Working Group regarding interpretation of metabolism images in early post-infarction patients: It has been the experience of some members of the Working Group that in early post-infarction patients (1-2 weeks), overestimation of FDG uptake may occur. This may be related to intense glycolytic activity of leukocytes in the necrotic zones of the myocardial infarction. Alternatively, FDG uptake may be lower than perfusion (reverse mismatch) especially in early post-infarction patients after thrombolysis. This may lower the predictive value of PET perfusion-metabolism imaging after an acute myocardial infarction and should be stated accordingly in the report.

RV uptake. When tracer activity concentrations are increased in the RV myocardium, they should be reported. The normal RV myocardial activity concentrations of FDG images are about 50% of those of the LV myocardium. Increased RV uptake is indicative of RV hypertrophy or overload, usually as a result of pulmonary hypertension. On the other hand, an apparent increase in RV activity may only be relative because of diminished LV uptake of FDG. However, little if any information on the significance of increased RV FDG uptake either associated with a concordant increase in perfusion or in excess of RV perfusion is available, so the clinical relevance of such uptake patterns remains uncertain at present.

v. **Metabolism and extent of viability: Quantitative.** Quantitative analysis can supplement the visual interpretation. As with the perfusion images, quantitative analysis of myocardial metabolism requires display of the tomographic short-axis slices in a polar map format that provides an easily comprehensible representation of the extent and severity of perfusion and metabolic abnormalities, as well as their relationship.[54,55] The "raw" perfusion and FDG polar maps are normalized to myocardial regions with the highest perfusion. To identify myocardial regions with increases in FDG uptake relative to perfusion, the FDG polar maps are then compared with the perfusion map, resulting in a "difference" polar map. The patient's polar maps (perfusion, metabolism, and their difference) are then compared with corresponding reference polar maps of normal subjects. Depending on the degree of FDG uptake, hypoperfused regions are then categorized into normal, perfusion-metabolism mismatch, or perfusion-metabolism match. The quantitative measurements should appropriately sample all segments of the left ventricle. The quantitative analysis system should be validated by appropriate studies published in peer-reviewed journals. Generally, determination of the count difference between regional FDG and flow tracer uptake (usually expressed as counts in defect divided by counts in normal or maximal count zone) is preferable to determinations of ratios of regional FDG and flow tracer uptake (ie, FDG/Rb-82 ratios for each pixel). Such ratios are susceptible to regional statistical variations in count densities and to image noise.

Myocardial glucose utilization in absolute units of micromoles of glucose per minute per grams of myocardium. Quantitative estimates of myocardial glucose utilization have not been found to aid in the assessment or characterization of myocardial viability due to the variability in substrate utilization by the myocardium, even when FDG images are acquired during a hyperinsulinemic-euglycemic clamp.[42,45,46] Methods for deriving quantitative estimates of myocardial metabolism require acquisition of serial images.[36,41] Regions of interest are placed on the myocardium and the LV blood pool and are copied to all serially acquired images in order to generate myocardial tissue and blood pool time-activity curves. The time-activity curves are corrected for spillover of activity from the blood pool into the myocardium and for radioactive decay. The time-activity curves are then fitted with a validated tracer kinetic model, and estimates of regional myocardial glucose utilization are obtained in micromoles of glucose per minute per grams of myocardium. Measurements of glucose metabolic rates further require determination of glucose concentrations in arterial or arterialized venous blood. Similar to myocardial perfusion, parametric images and polar maps are also available for display of rates of regional myocardial glucose utilization. Regional metabolic rates on such parametric images are coded by a color scale and can be determined noninvasively for any myocardial region through regions of interest assigned to the polar map.[69]

vi. **Comparison of myocardial metabolism to perfusion.** The comparison of perfusion and metabolism images obtained with PET is relatively straightforward because both image sets are attenuation-corrected. Thus, relative increases or decreases in myocardial metabolism relative to perfusion generally reflect the presence or absence of metabolic viability.

Special considerations for combining SPECT perfusion with PET metabolism images. In current clinical practice, FDG PET images are often read in combination with SPECT myocardial perfusion images. The interpreting physician should be careful when comparing the non–attenuation-corrected SPECT images with attenuation-corrected FDG PET images. Myocardial regions showing an excessive reduction in tracer concentration as a result of attenuation artifacts, such as the inferior wall or the anterior wall in female subjects, may be interpreted as perfusion-metabolism mismatches, resulting in falsely positive perfusion-metabolism mismatches. Two approaches have proved

useful for overcoming this limitation. First, because assessment of viability is relevant only in myocardium with regional contractile dysfunction, gated SPECT or PET images offer means for determining whether apparent perfusion defects are associated with abnormal regional wall motion. Second, quantitative analysis with polar map displays that are compared with tracer- and gender-specific databases (for SPECT images) may be a useful aid to the visual interpretation. Neither approach is foolproof, so the use of attenuation-corrected PET images acquired on the same instrument to minimize these problems is clearly preferable.

For myocardial FDG images acquired with SPECT equipped with ultrahigh-energy collimators or with SPECT-like coincidence detection systems, additional problems may be encountered especially when the images are not corrected for photon attenuation.[70-72] Myocardial regions with severely reduced tracer activity concentrations due to attenuation artifacts on both perfusion and metabolism imaging, such as the inferior wall in men or the anterior wall in women, may be interpreted erroneously as perfusion-metabolism matches. Attenuation of the high-energy 511-keV photons is less than that for the 140-keV photons of Tc-99m or the 60- to 80-keV photons of Tl-201 so that attenuation artifacts are less prominent for FDG images and may result in an apparent mismatch. Furthermore, the lower spatial resolution of SPECT imaging systems for FDG imaging, especially when using high-energy photon collimation and then comparing with Tc-99m or Tl-201 images, causes apparent mismatches for small defects, at the base of the left ventricle, or at the edges or borders of large perfusion defects. Such artifacts resulting from the use of different photon energies can be avoided by using dedicated PET systems for both perfusion and metabolism imaging. Again, quantitative analysis through polar map displays with comparison to radiotracer- and gender-specific databases of normal may aid in the visual interpretation.

vii. **Integration of perfusion and metabolism results.** The combined evaluation of regional myocardial perfusion and FDG metabolism images allows identification of specific flow-metabolism patterns that are useful to differentiate viable from nonviable myocardium. It is useful to start with a functional assessment, ideally from gated PET or SPECT imaging, as dysfunctional segments are those suitable for evaluation of myocardial viability. If stress perfusion images as well as resting perfusion images are available, jeopardized myocardium can be distinguished from normal myocardium, and myocardium perfused normally at rest but dysfunctional as a result of repetitive stunning can be distinguished from myopathic or remodeled myocardium.

Differences in blood pool concentration of tracers can impact on the apparent match or mismatch of perfusion-FDG images. The separate adjustment of threshold and contrast settings can help compensate for these discrepancies.

Four distinct resting perfusion-metabolism patterns may be observed in dysfunctional myocardium[44,64,68,73-90]:

1. Normal blood flow associated with normal FDG uptake.
2. Reduced blood flow associated with preserved or enhanced FDG uptake (perfusion-metabolism mismatch).
3. Proportionally reduced blood flow and FDG uptake (perfusion-metabolism match).
4. Normal or near-normal blood flow with reduced FDG uptake (reversed perfusion-metabolism mismatch).

Some laboratories have added a fifth pattern, a mild perfusion-metabolism match in which the regional uptake of both the tracer of blood flow and of FDG is mildly to moderately reduced.[80,84] Because contractile function in such "mild" matches generally does not improve after revascularization, the pattern is subsequently included in the general category of perfusion-metabolism matches. The patterns of abnormal perfusion-metabolism and of perfusion-metabolism mismatch identify potentially reversible myocardial dysfunction, whereas the pattern of a perfusion-metabolism match identifies irreversible myocardial dysfunction.

If stress and rest perfusion imaging information is available, it is useful to add an estimate of the extent of stress-inducible ischemia in regions of normal resting perfusion and FDG uptake, in regions with matched resting perfusion-FDG defects, or in regions with resting perfusion FDG-metabolic mismatch. The simultaneous display of stress and rest perfusion and FDG metabolic images is most helpful but not available on all display workstations. In circumstances where only resting perfusion imaging is performed alongside FDG metabolic imaging, besides reporting on the extent of scar and extent of hibernating myocardium, it is useful to indicate that one cannot rule out stress-inducible ischemia.

In circumstances where only stress perfusion imaging is available in combination with FDG metabolic imaging, the following patterns can be found in segments with contractile dysfunction:

1. Stress perfusion defect with preserved FDG uptake indicates ischemically jeopardized tissue (but distinction between ischemia, stunning, and hibernation is no longer possible), but revascularization is needed anyway.
2. Stress perfusion defects without preserved FDG uptake indicate scar tissue, and revascularization is not needed.

The interpretation should include a description of the probability for the potential for improvement in regional contractile function and in LVEF after revascularization.

The potential for a post-revascularization improvement in contractile function is low for perfusion-metabolism matches, even if the regional reductions in perfusion and in FDG uptake are only mild or moderate. Conversely, the potential for improvements in regional contractile dysfunction is high if perfusion is normal, if both perfusion and FDG uptake are normal, or if FDG uptake is significantly greater than regional perfusion (mismatch). Finally, the potential of a post-revascularization improvement in the LVEF by at least 5 or more EF units is high if the mismatch affects 20% or more of the LV myocardium.[44,68]

Qualitative or semiquantitative approaches can be applied to the interpretation of perfusion-metabolism patterns. Consistent with the qualitative analysis of myocardial perfusion defects, as described under paragraphs 14 and 15, concordant regional reductions in perfusion tracer and in FDG uptake should be defined as matches. Their extent may be small (5%-10% of the left ventricle), moderate (15%-20% of the left ventricle), or large (>20% of the left ventricle). The severity of a match is similarly expressed as mild, moderate, or severe. Regional uptake of FDG in excess of the reduced perfusion in the same myocardial region is interpreted as a mismatch. Depending on the difference between the uptakes of both tracers, the magnitude of a mismatch can be defined qualitatively as low, moderate, and high. Important for relating the FDG to the perfusion images is to define the myocardial region or segment that is normal. It is identified best on the perfusion images as the myocardium with the highest perfusion tracer uptake. Depending on the study conditions and the dietary state, the uptake of FDG in this region may be highest but also may be diminished or absent.

Semiquantitative assessments of perfusion and metabolism patterns may also be helpful. Similar to the scoring of perfusion defects and stress-rest perfusion differences, numerical scores can be applied to matches and mismatches. Identical scores for perfusion and FDG uptakes are consistent with matches. In contrast, at least one score difference in scores between the regional FDG uptake and perfusion tracer uptake should be considered as a mismatch. Again, it is important for the scoring approach to use the perfusion images for defining the normal myocardium. The segmental scores on the FDG images should be normalized to the perfusion scores (ie, the scores need to be adjusted so that scores in normal myocardium will be 0). The normalization approach and calculation of difference scores are depicted in Figure 2.

Critical for prediction of the potential for an improvement in global LV function is the number of segments with scores of mismatches. On the basis of the 17-segment model, four or more mismatch segments (or about 20% of the left ventricle) might be considered as predictive for a potential improvement in LV function after revascularization. Current evidence has not verified that the magnitude of a mismatch or the difference score serves as a predictor of the degree of functional improvement.

Reverse mismatch. A pattern of normal perfusion associated with reduced FDG uptake may be observed.[90-93] In most circumstances this results from a lack of or incomplete normalization of the myocardial FDG uptake. It has also been observed in patients with multivessel CAD, in patients with left bundle branch block, in patients after coronary angioplasty and thrombolysis, and in patients with diabetes. When observed, it is important to consider possible technical explanations for this pattern, such as inadequate or insufficient normalization of the image data. An important consideration for the interpretation of the "true" reverse mismatch is that perfusion is generally normal, suggesting that such regions, when dysfunctional, are viable. Although comments on the presence of such reverse mismatch may be made in the report, it is generally not advisable to include its relevance in the final impression, as it might lead to confusion.

Interpretation of FDG images when perfusion images have not been obtained. Interpretation of FDG images without perfusion images and/or angiographic information and/or without information on regional wall motion can be difficult and unreliable. This approach is not recommended for several reasons:

1. The presence of relatively well-preserved FDG uptake in dysfunctional myocardium does not differentiate an ischemic from a nonischemic process.
2. Regional absence and, conversely, regional increases in FDG uptake alone do not distinguish between normal and irreversibly injured myocardium. For example, uptake would be low in normal myocardium but increased in dysfunctional myocardium when studies are performed after more than 6 hours of fasting. Conversely, in the glucose-loaded state, uptake is highest in normal myocardium but frequently reduced in dysfunctional myocardium.
3. The degree of FDG accumulation over and above regional perfusion helps to assess the relative amount of scar and metabolically viable myocardium. The latter information may significantly influence the power of the test for predicting functional recovery. It is therefore recommended that FDG metabolic images be analyzed in combination with perfusion images obtained either with SPECT or, preferably, with PET.

F. Gated Myocardial FDG PET Images

Different from gated myocardial perfusion imaging with SPECT, the clinical usefulness of gated FDG PET is less firmly established, although parameters of global and regional function derived from gated PET have been found to correlate closely with those obtained through standard

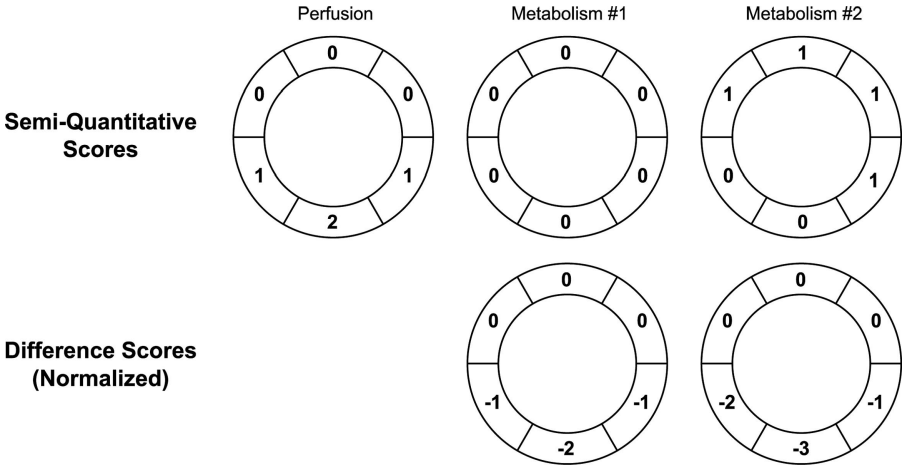

Figure 2. Semiquantitative scoring of metabolism images relative to perfusion images. The segmental perfusion and metabolism tracer uptake is shown schematically on a short-axis slice. Examples of two conditions are schematically depicted on short-axis slices, one with FDG uptake being highest in the normally perfused myocardium and one with FDG uptake being highest in the hypoperfused myocardium. As seen in the *upper panel*, FDG uptake on the metabolism No. 1 image in segments with normal perfusion scores (scores of 0) in the *top left panel* is scored with a 0, reflecting the highest uptake. The perfusion scores in the inferior wall of 1 and 2 (*top left panel*) reflect the mildly to moderately diminished perfusion. FDG uptake in these segments is normal and, hence, scored as 0. Metabolism perfusion difference scores are obtained by subtracting the perfusion scores from the metabolism scores; as depicted below the metabolism No. 1 images, the difference scores are −1 and −2 and reflect a perfusion-metabolism mismatch. In contrast, the metabolism No. 2 image schematically depicts an example of the highest FDG uptake in the hypoperfused inferior wall (again in comparison to the perfusion scores shown in the top left panel); the scores are therefore 0, whereas the scores of 1 in the normally perfused myocardium on the metabolism No. 2 image indicate the lower FDG uptake. Before deriving difference scores, the scores for the FDG uptake in the normal myocardium need to be normalized to those of perfusion (ie, they need to be set to 0). This is accomplished by subtracting a value of −1 from all segments on the FDG images so that the scores in the normally perfused myocardium become 0. The normalized scores for FDG uptake in the hypoperfused segments then become 0 and −1, and furthermore, the difference scores, as depicted in the *right lower panel*, are −1, −2, and −3. A difference score of 0 reflects normal or matched myocardial regions, and negative scores reflect a perfusion-metabolism mismatch.

techniques such as echocardiography, left ventriculography, and radionuclide angiography.[94-100] However, regional function can be more difficult to assess with gated FDG PET because of the prevalence of severe global LV dysfunction in patients referred for PET viability studies. In these patients, overall wall motion and thickening are likely to be poor and regional differences may therefore be only subtle. Nevertheless, because gated image acquisition can be performed at minimal expense, some incremental diagnostic information may be obtained at little if any additional cost. Display, analysis, and interpretation of gated PET myocardial perfusion and metabolism images should follow a structured and standardized approach. This approach should follow the guidelines published previously for gated SPECT perfusion imaging, as the methodologic aspects of gated PET as well as its diagnostic content are comparable to those of gated SPECT. The LV short-axis slices are divided into 17 segments (basal, mid, and distal) as proposed by American Heart Association/American College of Cardiology guidelines. These segments are scored for regional wall motion (scoring system: normokinesis, hypokinesis, akinesis, and dyskinesis). In the segments, the information on perfusion (stress-rest) and metabolism is integrated.

Findings on gated PET images if available may be included in the final report and may be interpreted within the context of the analysis of the images of perfusion and metabolism. LV volumes at end diastole and end systole and the LVEF, if available, should be included, as they contain independent diagnostic and prognostic information. In addition, evidence of contractile function can be helpful to identify stunning in dysfunctional myocardium with preserved perfusion and metabolism. Residual contractile function in areas of a moderate matched perfusion-metabolism defect may also aid in assessing the degree of viability and in predicting the magnitude of functional recovery after revascularization in such regions. Impaired function in areas of preserved resting perfusion and pre-

served FDG uptake without evidence of stress-induced perfusion defects suggests myopathic or remodeled myocardium. Nonetheless, further studies are needed to establish the incremental diagnostic value of gated PET.

G. Modification of the Interpretation by Relevant Clinical Information

With regard to perfusion imaging, the initial interpretation should be made without knowledge of the clinical characteristics and stress ECG findings. However, the final interpretation should be adjusted to some limited degree according to clinically relevant information. Age, pretest likelihood, history of known CAD, findings on the stress and rest electrocardiograms, and chest pain (of very limited significance after pharmacologic stress) all contain diagnostic and prognostic information that may impact the interpretation of the perfusion and viability study.

Similar to the guidelines for SPECT perfusion imaging, the adjusted interpretation should not vary from the initial assessment by more than one category of probability. For example, if the initial conclusion was "probably normal" (a 5-category scale as described above), the final interpretation could be changed to "equivocal" or "definitely normal," but it should not be re-categorized as "probably abnormal" or "definitely abnormal." The modification has the effect of improving the overall concordance of information sent to clinicians without substantially altering the information contained in the scintigraphic examination.

With regard to metabolism imaging, for the interpretation of the metabolic images, the integration of clinical information may be even more relevant. Angiographic data (if available) and rest and stress imaging results are relevant. Regional wall motion data from radionuclide angiography or 2D echocardiography can be critical for understanding findings on the metabolism images. In many cases it may be necessary to seek additional information from the referring clinician.

H. Reporting of PET Myocardial Perfusion-Metabolism Study Results

One is referred to a concurrently updated guideline on reporting.

i. **Patient information.** The report should start with the date of the study and then state the patient's age, sex, height, and weight or body surface area, as well as the patient's medical identification number.

ii. **Indication for study.** Stating the reasons for performing the study aids in focusing the study interpretation on the clinical question asked by the referring clinician. In addition, a clear statement of the reasons for the study has become critical for billing purposes.

iii. **History and key clinical findings.** A brief description of the patient's clinical history and findings can contribute to a more appropriate and comprehensive interpretation of the rest (and stress) perfusion and of the metabolism images. This information may include past myocardial infarctions and their location, revascularization procedures, the patient's angina-related and congestive heart failure–related symptoms, presence of diabetes or hypertension, and other coronary risk factors. Information on regional and global LV function can similarly be important for the interpretation of regional perfusion and metabolism patterns.

A description of the ECG findings may serve as an aid in the study interpretation, such as the presence of Q waves and their location or conduction abnormalities (eg, left bundle branch block) for exploring septal perfusion and/or metabolic abnormalities.

iv. **Type of study.** The imaging protocols should be stated concisely. This should include the type of imaging of myocardial perfusion and of myocardial metabolism with, for example, a PET or PET/CT system or SPECT perfusion and FDG PET metabolism imaging. If stress perfusion imaging was performed, this should be stated accordingly, indicating the type of stress, such as treadmill, dipyridamole, or adenosine. Radiopharmaceuticals used for the perfusion and the metabolism imaging studies should be stated, and their radioactivity doses should be given. The acquisition modes and image sequences should be described, such as static or dynamic image acquisition, for stress and rest perfusion imaging, perfusion and metabolism imaging on different days, and the use of gating.

The main body of the report following this introductory descriptive information should then be tailored to the specific clinical question asked by the referring clinician and the procedural approach chosen for answering this question. For example, the report for a stress-rest myocardial PET perfusion study will be different from a report describing and interpreting a myocardial perfusion and myocardial metabolism study. Furthermore, the report will again be different for a study that includes a stress and rest myocardial perfusion study and a myocardial metabolism study.

v. **Summary of stress data.** If myocardial perfusion has been evaluated during stress, the type of stress should be indicated (eg, physical or pharmacologic). In instances of pharmacologic stress, the agent should be described, as should the dose and route of administration. Side effects and symptoms experienced during stress should be indicated. If pharmacologic stress was discontinued prematurely, the reasons should be indicated.

The report should contain additional details on the stress study including changes in heart rate and blood pressure, occurrence of arrhythmias or conduction abnormalities, and development of ST-segment changes and their location. Type of chest pain during pharmaco-

logic stress has limited predictive value for myocardial ischemia, but whether it resembles chest pain from prior history should be noted, and its severity (mild, moderate, or severe) should be reported.

vi. **Summary of clinical laboratory data and dietary state.** Information on the dietary state (eg, fasting or post-prandial) and on interventions for manipulating plasma glucose levels through, for example, oral or IV administration of glucose or use of the euglycemic hyperinsulinemic clamp should be given. If pharmacologic measures, such as nicotinic acid derivatives, have been used, this should be described. Furthermore, BG levels, if obtained at baseline or after intervention, should be listed, as they are useful for the interpretation of the metabolic images.

vii. **Image description and interpretation: Perfusion images.** A statement regarding image quality is important. Reduced quality may affect interpretation or the confidence the interpreter has in the accuracy of the findings. If the cause of the reduced quality is known or suspected, then this should be stated accordingly. This information may prove useful when repeat images are obtained in the same patient.

The pretest likelihood of CAD may be determined with available algorithms that rely on parameters including age, sex, character of chest pain, number of coronary risk factors, and findings of stress electrocardiography. The findings on the stress/rest myocardial perfusion images are then included in order to derive a probability of CAD. An estimate of the probability may be reported based on the definite presence or absence of a perfusion defect, its extent and severity, and its change from stress to rest. Other findings such as a stress-related transient LV dilation should be included. When the presence of CAD has already been established, then the likelihood of stress-induced ischemia should be reported instead of the likelihood of significant CAD.

NOTE: It is acknowledged that in contrast to the extensive experience with SPECT myocardial perfusion imaging and the accordingly large body of evidence reported in the scientific literature, the experience with PET myocardial perfusion imaging is more limited. It seems acceptable, however, to extrapolate predictive information from the SPECT literature for assessing the probability of CAD or of stress-induced myocardial ischemia as well as assessment of cardiac risk through myocardial perfusion imaging. Nevertheless, such extrapolations should be made with caution because of methodologic differences in PET and SPECT for assessing the relative distributions of myocardial perfusion and its disease-related alterations.

When the report includes a quantitative estimate of regional myocardial blood flows, it should be given in milliliters per minute per grams of myocardium, describe changes in flow from rest to pharmacologically induced hyperemic stress, and be related to the specific clinical question to be answered. It is also useful to include estimates of regional myocardial flow reserve, as there is greater familiarity with this particular index. Normal values for myocardial perfusion reserves and for resting and hyperemic myocardial blood flows should be given for comparison. Estimates of myocardial blood flow at rest should also be related to the rate-pressure product as an index of cardiac work, an important determinant of resting myocardial blood flow, which could influence the apparent coronary flow reserve capacity (ability to augment flow during stress).

viii. **Image description and interpretation: Metabolism.** The report should describe the relative distribution of myocardial blood flow at rest and the location, extent, and severity of regional perfusion defects. The report should continue with a description of the FDG uptake in the myocardium and indicate the tracer activity concentrations in normally perfused and in hypoperfused myocardium. The glucose utilization state as evident from the radiotracer uptake in normally perfused myocardium and also from blood pool activity should then be reported and be related to the dietary state or the presence of insulin resistance (including impaired glucose tolerance and type 2 diabetes). This should be related to the residual blood pool activity as additional evidence for inadequate clearance of FDG from blood into tissue and provide the information for low tracer uptake in normally perfused myocardium. The regional FDG concentrations in hypoperfused myocardial regions should be described and categorized into perfusion-metabolism mismatches or matches. An estimate of the degree of mismatch (or the difference between FDG uptake and perfusion) and, more importantly, of the extent of a mismatch or match, or both, when present, should be given. Findings on semiquantitative or quantitative image analysis approaches may be added. Location and, in particular, extent of matches and mismatches are important because they contain prognostic information on future cardiac events and predictive information on potential outcomes in regional and global LV function, congestive heart failure–related symptoms, and long-term survival after revascularization. Finally, the description of the perfusion-metabolism findings may include a correlation to regional wall motion abnormalities and should indicate the potential for a post-revascularization improvement in the regional and global LV function.

ix. **Final interpretation.** Results should be succinctly summarized first to address the clinical question being asked, such as whether there is evidence of CAD or evidence of myocardial viability. Potential confounding effects of image artifacts or other quality concerns should be stressed in the summary. It is useful to conclude with a summary of the percentage of the LV muscle mass that is viable, as well as the percentage that shows the potential for ischemia.

The results should be compared with available prior

study results and any diagnostic changes in the interim highlighted. If possible, an estimate of the likelihood of CAD in instances of perfusion images or of the predicted outcome in regional or global LV function after revascularization should be provided. If additional diagnostic clarification seems needed, the physician may recommend an alternative modality.

References

1. Bacharach SL, Bax JJ, Case J, et al. PET myocardial glucose metabolism and perfusion imaging: part 1—guidelines for patient preparation and data acquisition. J Nucl Cardiol 2003;10:543-54.
2. Schelbert HR, Beanlands R, Bengel F, et al. PET myocardial perfusion and glucose metabolism imaging: part 2—guidelines for interpretation and reporting. J Nucl Cardiol 2003;10:557-71.
3. Beanlands RSB, Muzik O, Melon P, et al. Noninvasive quantification of regional myocardial flow reserve in patients with coronary atherosclerosis using nitrogen-13 ammonia positron emission tomography. Determination of extent of altered vascular reactivity. J Am Coll Cardiol 1995;26:1465-75.
4. Bergmann SR. Quantification of myocardial perfusion with positron emission tomography. In: Sobel BE, editor. Positron emission tomography of the heart. Mount Kisco (NY): Futura; 1992. p. 97-127.
5. Cardiogen-82 rubidium Rb-82. Princeton (NJ): Bracco Diagnostics; 2000.[package insert]
6. Choi Y, Huang SC, Hawkins RA, et al. A simplified method for quantification of myocardial blood flow using nitrogen-13-ammonia and dynamic PET. J Nucl Med 1993;34:488-97.
7. Hutchins GD, Schwaiger M, Rosenspire KC, et al. Noninvasive quantification of regional blood-flow in the human heart using N-13 ammonia and dynamic positron emission tomographic imaging. J Am Coll Cardiol 1990;15:1032-42.
8. Krivokapich J, Smith GT, Huang SC, et al. ^{13}N ammonia myocardial imaging at rest and with exercise in normal volunteers. Quantification of absolute myocardial perfusion with dynamic positron emission tomography. Circulation 1989;80:1328-37.
9. Schwaiger M, Ziegler SI, Bengel FM. Assessment of myocardial blood flow with positron emission tomography. In: Shaw PM, editor. Imaging in cardiovascular disease. Philadelphia: Lippincott Williams and Wilkins; 2000. p. 195-212.
10. Schoder H, Schelbert HR. Positron emission tomography for the assessment of myocardial viability: noninvasive approach to cardiac pathophysiology. In: Dilsizian V, editor. Myocardial viability: a clinical and scientific treatise. Armonk (NY): Futura; 2000. p. 391-418.
11. Schelbert HR. F-18-deoxyglucose and the assessment of myocardial viability. Semin Nucl Med 2002;32:60-9.
12. Shoder H, Schelbert HR. Positron emission tomography for the assessment of myocardial viability. In: Dilsizian V, editor. Myocardial viability: a clinical and scientific treatise. Armonk (NY): Futura; 2000. p. 391-418.
13. Di Carli M. Advances in positron emission tomography. J Nucl Cardiol 2004;11:719-32.
14. Kamel E, Hany TF, Burger, et al. CT vs 68GE attenuation correction in a combined PET/CT system: evaluation of the effect of lowering the CT tube current. Eur J Nucl Med Mol Imaging 2002;29:346-50.
15. National Electrical Manufacturers Association. NEMA standards publication NU 2-2001: performance measurements of positron emission tomographs. Washington, DC: National Electrical Manufacturers Association; 2001.
16. Schelbert HR, Phelps ME, Huang SC, MacDonald NS, Hansen H, Selin C, et al. N-13 ammonia as an indicator of myocardial blood flow. Circulation 1981;63:1259-72.
17. DeGrado TR, Bergmann SR, Ng CK, Raffel DM. Tracer kinetic modeling in nuclear cardiology. J Nucl Cardiol 2000;7:686-700.
18. International Commission on Radiological Protection. Radiation dose to patients from radiopharmaceuticals. ICRP Publication 80. Ann ICRP 2000;28:113.
19. International Commission on Radiological Protection. Radiation dose to patients from radiopharmaceuticals. ICRP Publication 53. Ann ICRP 1988;18:62.
20. Kim SH, Machac J, Almeida O, et al. Optimization of rubidium-82 generator performance [abstract]. Clin Nucl Med 2004;29: 135P.
21. Meerdink DJ, Leppo JA. Experimental studies of the physiologic properties of technetium-99m agents: myocardial transport of perfusion imaging agents. Am J Cardiol 1990;66:9E-15E.
22. Leppo JA, Meerdink DJ. Comparison of the myocardial uptake of a technetium-labeled isonitrile analogue and thallium. Circ Res 1989;65:632-9.
23. Mack RE, Nolting DD, Hogancamp CE, et al. Myocardial extraction of Rb-86 in the rabbit. Am J Physiol 1959;197:1175-7.
24. Becker L, Ferreira R, Thomas M. Comparison of Rb-86 and microsphere estimates of left ventricular blood flow distribution. J Nucl Med 1977;15:969-73.
25. Selwyn AP, Allan RM, L'Abbate A, et al. Relation between regional myocardial uptake of rubidium-82 and perfusion: absolute reduction of cation uptake in ischemia. Am J Cardiol 1982;50:112-21.
26. Goldstein RA, Mullani NA, Marani SK, et al. Myocardial perfusion with rubidium-82. II. Effects of metabolic and pharmacological interventions. J Nucl Med 1983;24:907-15.
27. Schelbert HR, Ashburn WL, Chauncey DM, et al. Comparative myocardial uptake of intravenously administered radionuclides. J Nucl Med 1977;15:1092-1100.
28. Chow BJ, Ruddy TD, Dalipaj MM, et al. Feasibility of exercise rubidium-82 positron emission tomography myocardial perfusion imaging [abstract]. J Am Coll Cardiol 2003;41:428A.
29. Garcia EV, Bacharach SL, Mahmarian JJ, et al. Imaging guidelines for nuclear cardiology procedures: part 1. J Nucl Cardiol 1996;3:G1-46.
30. Hickey KT, Sciacca RR, Bokhari S, et al. Assessment of cardiac wall motion and ejection fraction with gated PET using N-13 ammonia. Clin Nucl Med 2004;29:243-8.
31. Schwaiger M, editor. Cardiac positron emission tomography. Boston: Kluwer Academic Publishers; 1996. p. 366.
32. Moser KW, Hsu BL, Cullom SJ, et al. Count-based attenuation maps reconstructed with a Bayesian algorithm for more efficient cardiac PET imaging [abstract]. J Nucl Med 2005;46:262p.
33. Loghin C, Sdringola S, Gould KL. Common artifacts in PET myocardial perfusion images due to attenuation-emission misregistration: clinical significance, causes, and solution. J Nucl Med 2004;45:1029-39.
34. Hsu BL, Moser KW, Cullom SJ, et al. Correction of imaging artifacts from implanted leads in cardiac PET/CT: a phantom evaluation [abstract]. J Nucl Med 2005;46:174p.
35. Difilippo FP, Brunken RC, Kaczur T, Jaber W. Artifacts from implanted leads in cardiac PET using CT-based attenuation correction [abstract]. J Nucl Card 2004;11:S23.
36. Hamacher K, Coenen HH, Stauocklin G. Efficient sterospecific synthesis of no-carrier-added 2-[F-18]-fluoro-2-deoxy-D-glucose using aminopolyether supported nucleophilic substitution. J Nucl Med 1986;27:235-8.

37. ACRP-53. CDE Dosimetry Services. 2001. Available from: URL: http://www.internaldosimetry.com/freedosestimates/adult/index.html. Accessed October 19, 2006.
38. Stabin MG, Stubbs JB, Toohey RE. Radiation dose estimates for radiopharmaceuticals. Radiation Internal Dose Information Center. Oak Ridge Institute of Science and Education, Oak Ridge, Tenn. Available from: URL:http://www.nrc.gov/reading-rm/doc-collections/nuregs/contract/cr6345/cr6345.pdf.
39. Package insert for Tc-99m sestamibi kit (Cardiolite). Oak Ridge (TN): Radiation Internal Dose Information Center, Oak Ridge Institute for Science and Education.
40. Gallagher BM, Ansari A, Atkins H, et al. Radiopharmaceuticals XXVII. F-18-labeled 2-deoxy-2-fluoro-D-glucose as a radiopharmaceutical for measuring regional myocardial glucose metabolism in vivo: tissue distribution and imaging studies in animals. J Nucl Med 1977;18:990-6.
41. Ratib O, Phelps ME, Huang SC, et al. Positron tomography with deoxyglucose for estimating local myocardial glucose metabolism. J Nucl Med 1982;23:577-86.
42. Choi Y, Brunken RC, Hawkins RA, et al. Factors affecting myocardial 2-[F-18] fluoro-2-deoxy-D-glucose uptake in positron emission tomography studies of normal humans. Eur J Nucl Med 1993;20:308-18.
43. Ohtake T, Yokoyama I, Watanabe T, et al. Myocardial glucose-metabolism in noninsulin-dependent diabetes-mellitus patients evaluated by FDG-PET. J Nucl Med 1995;36:456-63.
44. Schöder H, Campisi R, Ohtake T, et al. Blood flow-metabolism imaging with positron emission tomography in patients with diabetes mellitus for the assessment of reversible left ventricular contractile dysfunction. J Am Coll Cardiol 1999;33:1328-37.
45. Knuuti MJ, Nuutila P, Ruotsalainen U, et al. Euglycemic hyperinsulinemic clamp and oral glucose load in stimulating myocardial glucose utilization during positron emission tomography. J Nucl Med 1992;33:1255-62.
46. Vitale GD, deKemp RA, Ruddy TD, Williams K, Beanlands RS. Myocardial glucose utilization and optimization of (18)F-FDG PET imaging in patients with non-insulin-dependent diabetes mellitus, coronary artery disease, and left ventricular dysfunction. J Nucl Med 2001;42:1730-6.
47. Streeter J, Churchwell K, Sigman S, et al. Clinical glucose loading protocol for F-18 FDG myocardial viability imaging [abstract]. Mol Imaging Biol 2002;4:192.
48. Martin WH, Jones RC, Delbeke D, Sandler MP. A simplified intravenous glucose loading protocol for fluorine-18 fluorodeoxyglucose cardiac single-photon emission tomography. Eur J Nucl Med 1997;24:1291-7.
49. Bax JJ, Veening MA, Visser FC, et al. Optimal metabolic conditions during fluorine-18 fluorodeoxyglucose imaging; a comparative study using different protocols. Eur J Nucl Med 1997;24:35-41.
50. DeFronzo RA, Tobin JD, Andres R. Glucose clamping technique: a method for quantifying insulin secretion and resistance. Am J Physiol 1979;237:E214-23.
51. Port SC, Berman DS, Garcia EV, et al. Imaging guidelines for nuclear cardiology procedures. J Nucl Cardiol 1999;6:G47-84.
52. Gambhir SS, Schwaiger M, Huang SC, et al. Simple noninvasive quantification method for measuring myocardial glucose utilization in humans employing positron emission tomography and fluorine-18 deoxyglucose. J Nucl Med 1989;30:359-66.
53. Porenta G, Kuhle W, Czernin J, et al. Semiquantitative assessment of myocardial blood flow and viability using polar map displays of cardiac PET images. J Nucl Med 1992;33:1628-36.
54. Nekolla SG, Miethaner C, Nguyen N, Ziegler SI, Schwaiger M. Reproducibility of polar map generation and assessment of defect severity and extent assessment in myocardial perfusion imaging using positron emission tomography. Eur J Nucl Med 1998;25:1313-21.
55. McCord ME, Bacharach SL, Bonow RO, et al. Misalignment between PET transmission and emission scans: its effect on myocardial imaging. J Nucl Med 1992;33:1209-14, discussion 1214-5.
56. Bettinardi V, Gilardi MC, Lucignani G, et al. A procedure for patient repositioning and compensation for misalignment between transmission and emission data in PET heart studies. J Nucl Med 1993;34:137-42.
57. Laubenbacher C, Rothley J, Sitomer J, et al. An automated analysis program for the evaluation of cardiac PET studies: initial results in the detection and localization of coronary artery disease using nitrogen-13-ammonia. J Nucl Med 1993;34:968-78.
58. Gould KL, Martucci JP, Goldberg DI, et al. Short-term cholesterol lowering decreases size and severity of perfusion abnormalities by positron emission tomography after dipyridamole in patients with coronary artery disease. A potential noninvasive marker of healing coronary endothelium. Circulation 1994;89:1530-8.
59. Krivokapich J, Stevenson LW, Kobashigawa J, Huang SC, Schelbert HR. Quantification of absolute myocardial perfusion at rest and during exercise with positron emission tomography after human cardiac transplantation. J Am Coll Cardiol 1991;18:512-7.
60. Kuhle WG, Porenta G, Huang SC, et al. Quantification of regional myocardial blood flow using ^{13}N-ammonia and reoriented dynamic positron emission tomographic imaging. Circulation 1992;86:1004-17.
61. Muzik O, Beanlands RS, Hutchins GD, et al. Validation of nitrogen-13-ammonia tracer kinetic model for quantification of myocardial blood flow using PET. J Nucl Med 1993;34:83-91.
62. Blanksma PK, Willemsen AT, Meeder JG, et al. Quantitative myocardial mapping of perfusion and metabolism using parametric polar map displays in cardiac PET. J Nucl Med 1995;36:153-8.
63. Dorbala S, Limaye A, Samson U. Normal and abnormal responses of left ventricular ejection fraction during vasodilator stress Rb-82 positron emission tomography (PET/CT) [abstract]. J Nucl Med 2005;46:P268.
64. Tamaki N, Yonekura Y, Yamashita K, et al. Prediction of reversible ischemia after coronary artery bypass grafting by positron emission tomography. J Cardiol 1991;21:193-201.
65. Mäki M, Luotolahti M, Nuutila P, et al. Glucose uptake in the chronically dysfunctional but viable myocardium. Circulation 1996;93:1658-66.
66. Gropler RJ, Siegel BA, Lee KJ, et al. Nonuniformity in myocardial accumulation of fluorine-18-fluorodeoxyglucose in normal fasted humans [see comments]. J Nucl Med 1990;31:1749-56.
67. Pagano D, Townend JN, Littler WA, et al. Coronary artery bypass surgery as treatment for ischemic heart failure: the predictive value of viability assessment with quantitative positron emission tomography for symptomatic and functional outcome. J Thorac Cardiovasc Surg 1998;115:791-9.
68. Gerber BL, Ordoubadi FF, Wijns W, et al. Positron emission tomography using (18)F-fluoro-deoxyglucose and euglycaemic hyperinsulinaemic glucose clamp: optimal criteria for the prediction of recovery of post-ischaemic left ventricular dysfunction. Results from the European Community Concerted Action Multicenter study on use of (18)F-fluoro-deoxyglucose positron emission tomography for the detection of myocardial viability. Eur Heart J 2001;22:1691-701.
69. Choi Y, Hawkins RA, Huang SC, et al. Parametric images of myocardial metabolic rate of glucose generated from dynamic

cardiac PET and 2-[^{18}F]fluoro-2-deoxy-d-glucose studies. J Nucl Med 1991;32:733-8.
70. Bax JJ, Visser FC, van Lingen A, Visser CA, Teule GJ. Myocardial F-18 fluorodeoxyglucose imaging by SPECT. Clin Nucl Med 1995;20:486-90.
71. Bax JJ, Visser FC, Cornel JH, et al. Improved detection of viable myocardium with fluorodeoxyglucose-labeled single-photon emission computed tomography in a patient with hibernating myocardium: comparison with rest-redistribution thallium 201-labeled single-photon emission computed tomography. J Nucl Cardiol 1997;4:178-9.
72. Bax JJ, Wijns W. Fluorodeoxyglucose imaging to assess myocardial viability: PET, SPECT or gamma camera coincidence imaging? J Nucl Med 1999;40:1893-5.
73. Tillisch J, Brunken R, Marshall R, et al. Reversibility of cardiac wall-motion abnormalities predicted by positron tomography. N Engl J Med 1986;314:884-8.
74. Marwick TH, Hollman J. Acute myocardial infarction associated with intravenous dipyridamole for rubidium-82 PET imaging. Clin Cardiol 1990;13:230-1.
75. Carrel T, Jenni R, Haubold-Reuter S, et al. Improvement of severely reduced left ventricular function after surgical revascularization in patients with preoperative myocardial infarction. Eur J Cardiothorac Surg 1992;6:479-84.
76. Lucignani G, Paolini G, Landoni C, et al. Presurgical identification of hibernating myocardium by combined use of technetium-99m hexakis 2-methoxyisobutylisonitrile single photon emission tomography and fluorine-18 fluoro-2-deoxy-D-glucose positron emission tomography in patients with coronary artery disease. Eur J Nucl Med 1992;19:874-81.
77. Tamaki N, Kawamoto M, Takahashi N, et al. Prognostic value of an increase in fluorine-18 deoxyglucose uptake in patients with myocardial infarction: comparison with stress thallium imaging. J Am Coll Cardiol 1993;22:1621-7.
78. Maes A, Flameng W, Nuyts J, et al. Histological alterations in chronically hypoperfused myocardium. Correlation with PET findings. Circulation 1994;90:735-45.
79. Paolini G, Lucignani G, Zuccari M, et al. Identification and revascularization of hibernating myocardium in angina-free patients with left ventricular dysfunction. Eur J Cardiothorac Surg 1994;8:139-44.
80. Schwarz E, Schaper J, vom Dahl J, et al. Myocardial hibernation is not sufficient to prevent morphological disarrangements with ischemic cell alterations and increased fibrosis. Circulation 1994; 90:I-378.
81. vom Dahl J, Eitzman D, Al-Aouar A, et al. Relation of regional function, perfusion, and metabolism in patients with advanced coronary artery disease undergoing surgical revascularization. Circulation 1994;90:2356-66.
82. Depré C, Vanoverschelde JL, Melin JA, et al. Structural and metabolic correlates of the reversibility of chronic left ventricular ischemic dysfunction in humans. Am J Physiol 1995;268: H1265-7.
83. Maes A, Flameng W, Borgers M, et al. Regional myocardial blood flow, glucose utilization and contractile function before and after revascularization and ultrastructural findings in patients with chronic coronary artery disease. Eur J Nucl Med 1995;22:1299-305.
84. vom Dahl J, Altehoefer C, Sheehan F, et al. Recovery of regional left ventricular dysfunction after coronary revascularization: impact of myocardial viability assessed by nuclear imaging and vessel patency at follow-up angiography. J Am Coll Cardiol 1996;28:948-58.
85. Flameng WJ, Shivalkar B, Spiessens B, et al. PET scan predicts recovery of left ventricular function after coronary artery bypass operation. Ann Thorac Surg 1997;64:1694-701.
86. Bax JJ, Visser FC, van Lingen A, et al. Metabolic imaging using F18-fluorodeoxyglucose to assess myocardial viability. Int J Card Imaging 1997;13:145-55, discussion 157-60.
87. Haas F, Haehnel CJ, Picker W, et al. Preoperative positron emission tomographic viability assessment and perioperative and postoperative risk in patients with advanced ischemic heart disease [see comments]. J Am Coll Cardiol 1997;30:1693-700.
88. Beanlands RS, Hendry PJ, Masters RG, et al. Delay in revascularization is associated with increased mortality rate in patients with severe left ventricular dysfunction and viable myocardium on fluorine 18-fluorodeoxyglucose positron emission tomography imaging. Circulation 1998;98:II51-6.
89. Fath-Ordoubadi F, Pagano D, Marinho NV, et al. Coronary revascularization in the treatment of moderate and severe postischemic left ventricular dysfunction. Am J Cardiol 1998; 82:26-31.
90. Bax JJ, Poldermans D, Elhendy A, et al. Improvement of left ventricular ejection fraction, heart failure symptoms and prognosis after revascularization in patients with chronic coronary artery disease and viable myocardium detected by dobutamine stress echocardiography. J Am Coll Cardiol 1999;34:163-9.
91. Maes A, Van de Werf F, Nuyts J, et al. Impaired myocardial tissue perfusion early after successful thrombolysis. Impact on myocardial flow, metabolism, and function at late follow-up. Circulation 1995;92:2072-8.
92. Maes A, Mortelmans L, Nuyts J, et al. Importance of flow/metabolism studies in predicting late recovery of function following reperfusion in patients with acute myocardial infarction. Eur Heart J 1997;18:954-62.
93. Yamagishi H, Akioka K, Hirata K, et al. A reverse flow-metabolism mismatch pattern on PET is related to multivessel disease in patients with acute myocardial infarction. J Nucl Med 1999;40:1492-8.
94. Yamashita K, Tamaki N, Yonekura Y, et al. Quantitative analysis of regional wall motion by gated myocardial positron emission tomography: validation and comparison with left ventriculography. J Nucl Med 1989;30:1775-86.
95. Yamashita K, Tamaki N, Yonekura Y, et al. Regional wall thickening of left ventricle evaluated by gated positron emission tomography in relation to myocardial perfusion and glucose metabolism. J Nucl Med 1991;32:679-85.
96. Boyd HL, Gunn RN, Marinho NV, et al. Non-invasive measurement of left ventricular volumes and function by gated positron emission tomography. Eur J Nucl Med 1996;23:1594-602.
97. Boyd HL, Rosen SD, Rimoldi O, Cunningham VJ, Camici PG. Normal values for left ventricular volumes obtained using gated PET. G Ital Cardiol 1998;28:1207-14.
98. Hor G, Kranert WT, Maul FD, et al. Gated metabolic positron emission tomography (GAPET) of the myocardium: ^{18}F-FDG-PET to optimize recognition of myocardial hibernation. Nucl Med Commun 1998;19:535-45.
99. Willemsen AT, Siebelink HJ, Blanksma PK, Paans AM. Automated ejection fraction determination from gated myocardial FDG-PET data. J Nucl Cardiol 1999;6:577-82.
100. Hattori N, Bengel FM, Mehilli J, et al. Global and regional functional measurements with gated FDG PET in comparison with left ventriculography. Eur J Nucl Med 2001;28: 221-9.